

SocialPulse: On-Device Detection of Social Interactions in Naturalistic Settings Using Smartwatch Multimodal Sensing

MD SABBIR AHMED*, Department of Systems and Information Engineering, University of Virginia, USA
KAITLYN DOROTHY PETZ, Department of Psychology, University of Virginia, USA
NOAH FRENCH, Department of Psychology, University of Virginia, USA
TANVI LAKHTAKIA, Department of Psychology, University of Virginia, USA
AAYUSHI SANGANI, Department of Psychology, University of Virginia, USA
MARK RUCKER, Department of Systems and Information Engineering, University of Virginia, USA
XINYU CHEN, Department of Systems and Information Engineering, University of Virginia, USA
BETHANY A. TEACHMAN, Department of Psychology, University of Virginia, USA
LAURA E. BARNES, Department of Systems and Information Engineering, University of Virginia, USA

Social interactions are fundamental to well-being, yet automatically detecting them in daily life—particularly using wearables—remains underexplored. Most existing systems are evaluated in controlled settings, focus primarily on in-person interactions, or rely on restrictive assumptions (e.g., requiring multiple speakers within fixed temporal windows), limiting generalizability to real-world use. We present an on-watch interaction detection system designed to capture diverse interactions in naturalistic settings. A core component is a foreground speech detector trained on a public dataset. Evaluated on over 100,000 labeled foreground speech and background sound instances, the detector achieves a balanced accuracy of 85.51%, outperforming prior work by 5.11%.

We evaluated the system in a real-world deployment (N=38), with over 900 hours of total smartwatch wear time. The system detected 1,691 interactions, 77.28% were confirmed via participant self-report, with durations ranging from under one minute to over one hour. Among correct detections, 81.45% were in-person, 15.7% virtual, and 1.85% hybrid. Leveraging participant-labeled data, we further developed a multimodal model achieving a balanced accuracy of 90.36% and a sensitivity of 91.17% on 33,698 labeled 15-second windows. These results demonstrate the feasibility of real-world interaction sensing and open the door to adaptive, context-aware systems responding to users' dynamic social environments.

Additional Key Words and Phrases: Social Interaction, On-Watch System, Foreground Speech, Interaction Cues, Audio, Multi-Modal Model

*Corresponding author

Authors' Contact Information: Md Sabbir Ahmed, msabbir@virginia.edu, Department of Systems and Information Engineering, University of Virginia, USA; Kaitlyn Dorothy Petz, kdp8y@virginia.edu, Department of Psychology, University of Virginia, USA; Noah French, njf5cu@virginia.edu, Department of Psychology, University of Virginia, USA; Tanvi Lakhtakia, lakhtakia@virginia.edu, Department of Psychology, University of Virginia, USA; Aayushi Sangani, cjv8xy@virginia.edu, Department of Psychology, University of Virginia, USA; Mark Rucker, mr2an@virginia.edu, Department of Systems and Information Engineering, University of Virginia, USA; Xinyu Chen, dfs3mc@virginia.edu, Department of Systems and Information Engineering, University of Virginia, USA; Bethany A. Teachman, bteachman@virginia.edu, Department of Psychology, University of Virginia, USA; Laura E. Barnes, lb3dp@virginia.edu, Department of Systems and Information Engineering, University of Virginia, USA.

Permission to make digital or hard copies of all or part of this work for personal or classroom use is granted without fee provided that copies are not made or distributed for profit or commercial advantage and that copies bear this notice and the full citation on the first page. Copyrights for components of this work owned by others than the author(s) must be honored. Abstracting with credit is permitted. To copy otherwise, or republish, or post on servers or to redistribute to lists, requires prior specific permission and/or a fee. Request permissions from permissions@acm.org.

© 2018 Copyright held by the owner/author(s). Publication rights licensed to ACM.

ACM XXXX-XXXX/2018/2-ART

<https://doi.org/XXXXXXXX.XXXXXXX>

ACM Reference Format:

Md Sabbir Ahmed, Kaitlyn Dorothy Petz, Noah French, Tanvi Lakhtakia, Aayushi Sangani, Mark Rucker, Xinyu Chen, Bethany A. Teachman, and Laura E. Barnes. 2018. SocialPulse: On-Device Detection of Social Interactions in Naturalistic Settings Using Smartwatch Multimodal Sensing. 1, 1 (February 2018), 32 pages. <https://doi.org/XXXXXXXX.XXXXXXX>

1 Introduction

Social interactions are an integral part of everyday life and play a key role in well-being [40, 53]. Positive interactions with others can lift mood and create a sense of meaning [55]. However, negative social interactions, or complete social avoidance, can also adversely affect health [67, 69], contributing to anxiety and depression [21, 63]. Being able to detect real-world social interactions may allow us to disrupt unhealthy interaction patterns as they occur, enabling personalized interventions that promote mental well-being in everyday life. More broadly, social interaction detection is a foundational capability for context-aware systems, allowing them to respond dynamically to users' changing social contexts.

One method for capturing information about social interactions and their patterns is through self-report data (e.g., [42, 70]). For example, an individual could be prompted periodically or at the end of the day to describe all their social interactions. While straightforward to collect using traditional survey methods, such data are impacted by retrospective bias and may be burdensome for participants to provide [44, 65]. A promising alternative is passive sensing, which can collect real-time data unobtrusively and with minimal user burden. Several studies have used smartphones to passively detect social interactions, but these are limited by small sample sizes (e.g., $N=5$ in [32]) and evaluations in controlled environments [29], raising concerns about generalizability. Further, smartphones may not collect high quality data important to interaction detection. For example, they are often stored in pockets, resulting in lower quality acoustic data [39]. In contrast, smartwatches are more consistently worn close to the body in different contexts and locations [68], which may make them more suitable for continuous interaction detection.

Despite growing interest in smartwatch-based social interaction detection, relatively few systems have been demonstrated and evaluated for real-time use in unconstrained, everyday settings, and existing approaches necessarily make design choices that shape their scope and applicability. For example, Liang et al. [39] present foundational work on a smartwatch system for detecting in-person social interactions, demonstrating the promise of on-watch sensing for social context inference. Their system focuses specifically on in-person interactions and adopts modeling assumptions—such as requiring the watch user with at least one other person within fixed temporal windows—that are well suited to certain conversational settings but may not generalize to others, including interactions with extended single-speaker segments, as well as virtual (e.g., phone or video calls) and hybrid interactions, in which participants engage with a combination of co-located and remote conversation partners, which have become an increasingly common part of daily life [26].

Other work has explored alternative sensing modalities, including physiological signals such as respiration, to detect conversational activity [6, 62]. While these approaches provide valuable insights into the relationship between physiology and social interaction, they face practical challenges for large-scale, real-world deployment. In particular, respiration sensors are not available on most commercially deployed smartwatches (e.g., Samsung Galaxy Watch [72]), and respiration rate estimates on devices such as Fitbit and Apple Watch are typically limited to sleep periods [5, 19], when social interactions are unlikely to occur.

To build on foundational smartwatch-based systems and address their limitations, we propose a social interaction detection system that operates on off-the-shelf Wear OS smartwatches and captures audio-based interactions across in-person, virtual, and hybrid settings. In addition to enabling real-time interaction detection, the system was explicitly designed to facilitate the collection of fine-grained, real-world interaction labels. To this end, we developed an initial prototype for automatic interaction detection (Section 3), where a core component is a foreground speech (i.e., speech of the watch user [2, 38]) detector (section 3.2).

The system supports participant-driven annotation by leveraging smartwatch-based ecological momentary assessments (EMAs) that are triggered when potential interaction start and end times are detected based on probability of foreground speech (section 3.4). This design directly addresses a key challenge in naturalistic data collection: users may forget or be unwilling to manually initiate or terminate recordings during everyday interactions. By prompting users at salient moments, the smartwatch serves both as a sensing platform and as a low-burden labeling interface. We deployed the system on smartwatches (Section 4) with 38 participants (Section 5) to evaluate detection performance while simultaneously collecting annotated interaction labels alongside multimodal sensor data (Section 4.1, e.g., photoplethysmography). To further improve label coverage, we employed multiple complementary annotation strategies, including periodic prompts to identify missed interactions (Section 4.2).

Results from the on-device deployment of our initial prototype (Section 5) show that participants used the system for a total of 120 days. During this period, the system automatically detected 1,691 interactions, achieving an interaction detection accuracy of 77.28% ($N = 1,299$), with an average per-participant accuracy of 79.56%. The correctly detected interactions spanned in-person, virtual, and hybrid settings and covered a wide range of durations—from brief interactions (approximately one minute) to extended interactions lasting over one hour—demonstrating the system’s ability to capture diverse social interactions in fully naturalistic settings. Building on these deployment results, we further developed a multimodal model (Section 6) that enables finer-grained interaction inference and achieves a balanced accuracy of 90.36% when evaluated on around 33,700 labeled 15-second windows collected in fully naturalistic settings.

Through this work, we contribute to the ubiquitous computing and human–computer interaction (HCI) communities in the following ways:

- **Improved foreground speech detection for on-device social sensing.** We introduce a foreground speech detector (FSD) that achieves a balanced accuracy of 85.51%, outperforming recent state-of-the-art approaches [2, 38] by approximately 5.11%. As foreground speech detection is a core building block for privacy-preserving social sensing tasks—including social interaction detection, social connection analysis, and network estimation—this improvement has broad applicability within ubiquitous computing systems.
- **A fully on-device, real-time system for social interaction detection in daily life.** We present and validate an end-to-end smartwatch-based system that detects social interactions in real-time using fully on-device inference and privacy-preserving sensing. Raw audio is processed transiently on-device and is neither stored permanently nor transmitted. We evaluate the system in a three-day real-world deployment with 38 participants, demonstrating reliable detection of *in-person*, *virtual*, and *hybrid* interactions ranging from approximately one minute to over one hour in duration. Compared to prior on-device interaction detection systems [39, 75], our system advances the state of the art in several important ways:
 - It operates without restrictive assumptions, such as requiring the watch user with at least one other person within fixed temporal windows.
 - To our knowledge, it represents the *largest real-world evaluation* of an on-watch interaction detection system to date, comprising over 900 hours of continuous smartwatch operation, compared to fewer than 50 hours in prior work [39].
 - It supports detection of in-person, virtual, and hybrid interactions, extending prior smartwatch-based approaches that primarily focus on in-person encounters [39, 75].
- **Resource efficient multimodal interaction detection system with strong accuracy–efficiency tradeoffs.** We introduce a multimodal interaction detection model that achieves a balanced accuracy 90.36% when evaluated on more than 900 hours of fully naturalistic data containing 33,698 samples. This represents improvements of 9.23% and 2.89% in balanced accuracy compared to models trained using MobileNetV1 [25] and a custom YAMNet-based [58] model, respectively. Importantly, the proposed multimodal system design is resource efficient and reduces resource consumption relative to existing approaches, enabling continuous,

real-time interaction detection on smartwatches *without requiring raw audio transmission, storage, or off-device processing*.

2 Related Work

Prior work on social interaction detection spans smartphone- and wearable-based systems. Many existing approaches, however, rely on continuous audio capture, off-device processing, or restrictive assumptions that limit privacy and real-world generalizability. Motivated by mental health applications requiring reliable, in-the-wild sensing under strict privacy and resource constraints, we organize related work by platform (smartphones vs. wearables) and sensing modality, emphasizing on-device feasibility, privacy, and modeling assumptions.

2.1 Interaction Detection Leveraging Smartphones

Early work on social interaction detection relied on custom-built devices prior to the widespread adoption of smartphones [9]. The emergence of smartphones enabled broader exploration of interaction sensing using embedded sensors, particularly audio. Several studies leveraged speech and voice activity detection to infer conversations and social interactions [32, 60, 65], with later systems integrating multimodal sensing [29]. Models proposed in early work [32, 60] informed the conversation detection module in the StudentLife project [71], which subsequently formed the basis of the AWARE framework [18] and has been widely adopted in phone-based studies [65].

Despite their influence, most smartphone-based approaches were evaluated using limited labeled data collected under controlled conditions [3, 43, 45] or very short naturalistic settings [45]), leaving their robustness in naturalistic settings unclear. In addition, these systems rely primarily on speech related features, which can reduce reliability in real-world contexts where speech is intermittent or absent. While non-speech vocalizations such as laughter may also indicate social interaction, they are typically not explicitly modeled. Taken together, smartphones, while pervasive, are not consistently on-person or uniquely associated with a single user and are often obstructed, whereas smartwatches are worn more continuously, can capture more interactions, and support higher notification response rates, making them better suited for reliable social sensing and low-burden interventions [30, 39, 59, 68].

2.2 Interaction Detection Leveraging Wearable Sensors

Prior work has explored wearable sensing for detecting conversational activity, including respiration-based bands [6, 62]. Several studies collected data in both controlled and real-world environments [6, 7]. Because labeling in-the-wild data is challenging, some work used speech segments detected by the LENA device as ground truth for interaction boundaries [6], later combining LENA with learned models [7]. However, LENA was originally designed for child speech and relies on simple Gaussian mixture models [64, 73], which limits its performance on adult populations. Recent evaluations report low recall (e.g., 62% [49]) for adult speaker recognition [34, 49]. Moreover, respiration-based systems typically require additional hardware such as chest straps [6, 62], which can be obtrusive and impractical for long-term, everyday use. These systems also lack scalability, as off-the-shelf smartwatches do not include respiration sensors, and commercial respiration estimates are generally limited to sleep contexts [5, 19].

To address these limitations, more recent work has investigated social sensing using commercially available smartwatches, which are widely adopted and comfortable for all-day wear. For example, [8] developed an on-watch speech detection system using 3.5 hours of data. However, speech alone is insufficient for reliable interaction detection: systems need to distinguish foreground speech from background or ambient audio [39]. Without this distinction, environmental sounds such as television audio or nearby conversations may be misclassified as

social interactions [32]. Consequently, foreground speech detection has emerged as a critical component of social interaction sensing.

Several models for foreground speech detection have been proposed [2, 38, 52]. However, some foreground speech-based interaction detection approaches impose assumptions that may not hold across all real-world contexts. For example, the system described in [39] assumes the presence of at least two speakers, including the watch user, within fixed temporal windows, potentially limiting performance in scenarios such as one-on-one meetings or lectures.

Beyond audio, prior work has explored additional sensing modalities for interaction inference. Physiological signals have been shown to differ between interaction and non-interaction contexts [27], and IMU data may provide complementary behavioral cues. A recent study combined acoustic and IMU sensing for social interaction detection [75], but similarly assumed presence of watch user with at least one other speaker within short windows and evaluated performance in semi-controlled, speech-centric settings. As a result, the generalizability of these approaches to unconstrained, naturalistic environments remains an open challenge.

3 Design of Social Interaction Detection Pipeline for In-the-Wild Annotation

Before collecting real-world participant data, we developed an initial social interaction detection system on off-the-shelf smartwatches using a publicly available dataset and pretrained model. The primary goal of this initial system was to support participant-driven annotation of detected interactions. Specifically, users were prompted via smartwatch notifications when the system automatically detected the start and end of a potential interaction.

In everyday settings, individuals are not accustomed to tracking social events at fine temporal granularity, and many interactions are spontaneous or unplanned, making it difficult to initiate data recording before an interaction begins. In this context, notifications triggered after a automatically detected interactions provide a practical and low-burden mechanism for enabling fine-grained annotation.

To complement these event-triggered prompts, we also periodically issued notifications (every 80–90 minutes) asking participants whether the system missed any interactions during the preceding interval and, if so, to provide the approximate corresponding start and end times. This combination of event-driven and periodic prompting was designed to reduce annotation burden while improving coverage of naturally occurring social interactions.

3.1 Defining and Operationalizing Social Interaction

We define social interaction as vocal engagement with others occurring in person or through virtual modalities (e.g., phone or video calls), consistent with prior work [76]. Unlike previous approaches that impose additional constraints such as stationary participants or continuous turn-taking speech [29], we do not require such restrictions to better capture the variety of real-world interactions that can occur.

Crucially, social interaction is not characterized by continuous speech alone. Paralinguistic vocal behaviors (e.g., laughter, shouting) and periods of silence may still reflect reciprocal engagement between individuals. Accordingly, our system does not require speech in every sensing window; instead, it operationalizes interaction using patterns of speech presence and interaction cues over time, allowing detection to better reflect naturalistic social behavior.

Although the definition of social interaction may overlap with conversation—where conversation is typically defined as “verbal interaction between two or more people” [74]—our system is designed to detect social interaction rather than conversation alone. Prior systems, such as [39, 75], focus on conversation detection using continuous sensing and require the presence of at least two speakers, including the watch wearer, within every 30-second window. We build on this foundational work, as such assumptions may not consistently hold in real-world

settings (e.g., during student–advisor meetings, storytelling where one individual speaks for extended periods, or situations where two friends talk while the watch user mainly listens and speaks later).

Instead of imposing a per-window requirement that the watch wearer speak during every 15-second sensing window, we require a minimum amount of foreground speech from the wearer aggregated over the duration of an interaction (e.g., across a 20-minute interval), better reflecting real-world interaction dynamics in which individual airtime varies substantially [10]. Moreover, the system incorporates a broader set of vocal interaction cues beyond speech alone, including laughter, shouting, and whispering, which must be present for at least 50% (details in Section 3.4.1) of each 15-second recording. During the remaining portion of each window, silence may occur in any sequence.

The system also employs duty-cycled sensing rather than continuous recording, collecting data for 15 seconds every 1 minute and 30 seconds. This design allows interaction-related behaviors—both verbal and non-verbal—to occur during unsensed intervals, further aligning detection with naturalistic patterns of social interaction. Together, these design choices introduce substantial flexibility and enable the system to capture situations in which individuals are socially engaged without actively conversing, thereby distinguishing social interaction detection from conversation detection alone.

Taken together, these choices move beyond conversation-centric assumptions and align with broader conceptualizations of social interaction [76]. This definition was provided to participants via the study user manual and was reviewed and discussed by a research assistant during the baseline study visit to ensure understanding and support accurate, consistent annotation.

3.2 Development and Evaluation of Foreground Speech Detection

3.2.1 Model Development. Consistent with our definition of social interaction as vocal-based engagement with other people [76], the presence of the watch wearer’s own speech constitutes a necessary signal for interaction detection. Accordingly, we developed a FSD that identifies speech produced by the watch wearer while treating all other audio—including speech from others, music, environmental sounds, and silence—as background [2, 38].

Dataset and constraints. We trained the model using a publicly available dataset [38] consisting of 1-second audio segments, each manually labeled as either foreground or background sound. The dataset contains a total of 113,820 instances, of which 76.29% ($N = 86,829$) are labeled as background sound and 23.71% ($N = 26,991$) as foreground speech.

One approach to foreground speech detection relies on hand-crafted acoustic features (e.g., MFCCs and chromagrams) [2]. While extracting multiple features on-device can support richer behavioral characterization and enable reuse across downstream tasks, such feature extraction can incur substantial computational overhead. For example, prior work reports that feature extraction required over 1.5 minutes for nearly every probe start [2], limiting its suitability for scenarios in which timely or continuous prediction is required.

Although classical machine learning models (e.g., decision trees) may train more efficiently than deep learning models, the feature-extraction stage remains computationally expensive and can also constrain predictive performance. Moreover, our objective is not to train models on-device. Instead, we train models offline and deploy them to smartwatches for real-time inference, explicitly minimizing on-device computation to support sustained, long-term operation on resource-constrained wearable devices.

In developing the deep learning model for FSD, we focused on leveraging transfer learning, as prior work has demonstrated its effectiveness in wearable and audio-based sensing tasks [1, 17] and suggests it may similarly benefit foreground speech identification. Prior FSD work [38], for example, adopted a transfer-learning approach using embeddings from pretrained models, including one trained on data of celebrities and another trained on a random subset of 100 individuals from a dataset comprising approximately five hours of audio. While effective,

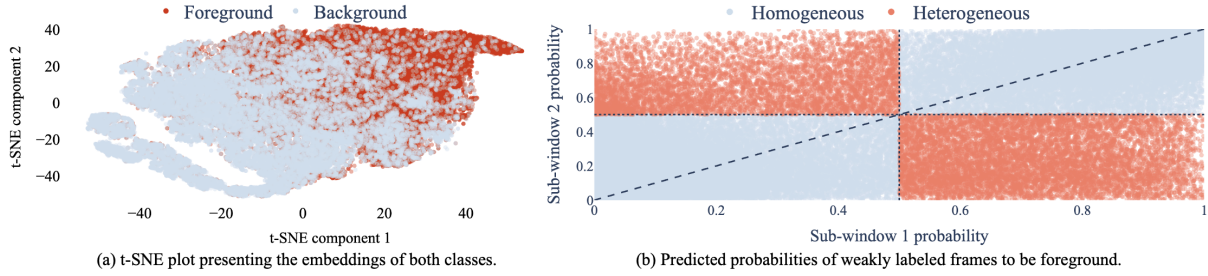


Fig. 1. Difference between foreground and background sound. (a) Visualization of embeddings for 50,000 audio frames (25,000 per class). For readability, embeddings for all 227,640 frames are not shown. (b) Predicted foreground speech probabilities for all frames. Homogeneous blocks indicate audio instances in which both sub-frames have predicted probabilities either above or below 50%, whereas heterogeneous blocks indicate instances in which the two sub-frames have opposite predictions (e.g., one sub-frame exceeds the 50% threshold while the other falls below it).

such training sources may limit generalizability, as they rely on non-representative training samples or relatively small datasets that may not reflect everyday wearable audio conditions.

Embedding-Based Modeling with Transfer Learning: To develop the FSD, we applied transfer learning by extracting embeddings from the YAMNet model [58]. YAMNet is a suitable choice because it is trained on 521 audio event classes (e.g., speech, laughter, music) from the large-scale AudioSet dataset [20, 22], which comprises 2.1 million YouTube videos totaling 5.8 thousand hours of audio. Training on such a large and diverse set of sound classes enables YAMNet to learn general-purpose audio representations. In addition, YAMNet is computationally efficient, with reported inference latency below 15 milliseconds (ms) [16].

By visualizing the embeddings of the dataset used to train the FSD model, we observed that YAMNet embeddings exhibit class-discriminative structure between foreground and background audio segments, but with substantial overlap (Figure 1(a)). This overlap suggests that simple linear decision boundaries are insufficient, motivating the use of a neural network model capable of learning non-linear relationships.

Accordingly, we developed a fully connected neural network classifier operating on the extracted embeddings to predict whether an audio instance corresponds to foreground speech or background sound. We used binary cross-entropy as the loss function and the Adam optimizer for training. To address class imbalance and ensure that the minority class received sufficient emphasis during learning, we applied class weighting using the formula $\text{weight}_c = \frac{1}{n_c} \cdot \frac{N}{2}$, where n_c denotes the number of instances in class c and N is the total number of instances. This weighting strategy balances the loss contributions across classes and mitigates bias toward the majority class.

The model was trained for 25 epochs, with early stopping applied when the validation loss did not improve for three consecutive epochs.

Weak Supervision and Meta-Learning. The dataset used to train the FSD model provides labels at the 1-second segment level. Each 1-second segment corresponds to two YAMNet frames, as YAMNet processes fixed 0.48-second windows regardless of input length. Although it may seem reasonable to train and evaluate models directly on these 0.48-second subwindows by assigning them the same label as the parent 1-second segment, this approach can be misleading. As noted in the dataset description [38], a 1-second segment is labeled as foreground speech if it contains either only the watch wearer’s speech or a mixture of the wearer’s and others’ speech. Consequently, individual subwindows within a mixed segment may not correspond to purely foreground speech. Assigning identical labels to such subwindows and using them for evaluation can therefore introduce label noise and distort performance estimates.

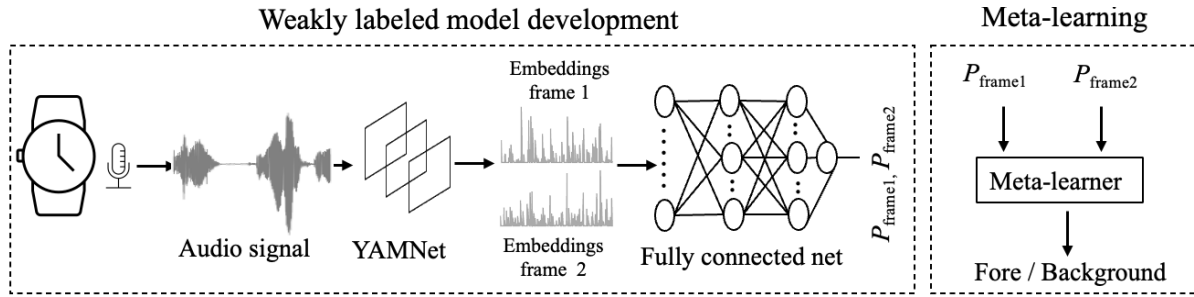


Fig. 2. The pipeline for on-watch foreground speech prediction. P_{frame1} and P_{frame2} denote the probabilities of foreground speech for frame 1 and frame 2, respectively.

To maintain consistency with the dataset’s instance-level labeling scheme while leveraging pretrained embeddings, we adopted a weak supervision strategy. Specifically, we assigned the 1-second label to each of the two subwindows and trained the deep learning model on these weakly labeled subwindows to obtain predicted probabilities for each frame. We then trained a meta-learner that used the two subwindow probability outputs as input features to produce a final classification for the full 1-second audio instance (foreground vs. background), which was used for model evaluation.

A straightforward alternative would be to determine the final class based solely on the direction of the subwindow predictions—for example, labeling an instance as foreground speech only if both subwindow probabilities exceed 0.5. However, as shown in Figure 1(b), many instances exhibit disagreement between the two subwindows (e.g., one probability above 0.5 and the other below). In such cases, a naive rule based only on prediction direction would fail to classify a substantial number of instances accurately, motivating the meta-learner. Accordingly, we evaluated multiple classification algorithms for the meta-learner, using the predicted subwindow probabilities as input features.

3.2.2 Model Evaluation and Baselines. For evaluation, we employed a stratified 10-fold cross-validation procedure. In each iteration, nine folds were used for training, while the remaining fold was split such that 10% of its samples were used for validation and 10% for testing. We repeated this process by swapping the validation and test subsets so that, across iterations, the entire fold was treated as test data. Importantly, the model was retrained from scratch for each split to prevent information leakage between the validation and test sets. To maximize the amount of training data, no validation samples were drawn from the nine training folds.

For the meta-learning stage, we maintained the same training and testing folds as those used for the weakly labeled model to ensure consistency and to avoid information leakage across learning stages.

To benchmark our foreground speech detection models, we compared against two existing approaches [2, 38], both of which were evaluated on the same publicly available dataset [38], enabling meaningful comparison. The method proposed by [38] employs a convolutional neural network–based architecture, whereas [2] uses classical machine learning models, such as Random Forests. In addition to using the same dataset, we adopted the same evaluation metrics—macro F1 score and balanced accuracy—as prior work [2, 38] to ensure a fair and comparable assessment.

3.2.3 Performance of the Foreground Speech Detector. We evaluated a diverse set of classification algorithms, including Decision Trees, K-Nearest Neighbors (KNN), and Logistic Regression, as candidates for the meta-learner trained on predicted probabilities from 113,820 audio instances labeled as foreground or background speech.

Among these approaches, a Nearest Centroid–based classifier [33] achieved the best performance, attaining a balanced accuracy of 85.51%.

By comparison, existing foreground speech detection models evaluated on the same dataset report balanced accuracies of 80.4% [38] and 80.3% [2]. Our approach therefore improves balanced accuracy by at least 5.11%.

Algorithm	Precision	Sensitivity	Specificity	BA	F1
Meta-learner (DecisionTree)	75.98	63.50	88.56	76.03	76.00
Meta-learner (ExtraTrees)	80.42	66.94	91.47	79.21	79.78
Meta-learner (RandomForest)	81.04	67.58	91.82	79.70	80.33
Meta-learner (KNN)	81.04	68.23	91.67	79.95	80.47
Meta-learner (GradientBoost)	83.26	71.35	92.72	82.03	82.61
Meta-learner (MLP)	83.24	71.67	92.64	82.15	82.67
Meta-learner (Logit)	82.79	73.01	92.00	82.50	82.65
Meta-learner (LinearSVC)	82.36	75.75	91.01	83.38	82.85
Meta-learner (NearestCentroid)	80.21	84.86	86.16	85.51	82.14
Ahmed et al. 2024 [2]	73.0	85.3	75.2	80.3	74.0
Liang et al., 2023 [38]	NA	NA	NA	80.4	81.50

Table 1. Performance comparison of meta-learning algorithms used in the proposed framework and existing baseline models [2, 38]. Values in bold indicate the best-performing model in terms of balanced accuracy. BA: Balanced Accuracy; NA: Not Available.

3.2.4 Foreground Speech Detection Discussion. The improved performance of our foreground speech detection pipeline stems from two key design choices. First, we leverage YAMNet embeddings trained on thousands of hours of diverse audio data, providing a more robust and generalizable representation than prior approaches based on manually engineered features or datasets collected in constrained contexts [2, 20, 38]. Second, we introduce a meta-learning stage that jointly reasons over predictions from the two subwindows within each 1-second segment. As shown in Figure 1(b), subwindow-level predictions frequently disagree; rather than relying on a fixed threshold or naive aggregation rule, the meta-learner learns consistent patterns across frames, leading to more reliable foreground speech detection and a balanced accuracy of 85.51%.

3.3 Interaction Cue Detection

While FSD provides a critical signal for identifying social interaction, speech alone does not fully capture the range of behaviors that occur during everyday interactions. In many real-world settings, interactions may involve limited speech or be characterized by non-verbal and paralinguistic vocal cues, motivating the inclusion of additional interaction cues beyond foreground speech. To detect these cues, we leveraged the pretrained YAMNet model [58]. From these, we identified 12 classes as indicative of *interaction cues*.

Prior work [39] focused on a narrow subset of conversation-related classes, including *Conversation*, *Chatter*, and *Whispering*. Building on this, we retained these classes and additionally selected nine classes that capture a broader range of vocal and paralinguistic behaviors relevant to social interaction¹: *Speech*, *Shout*, *Screaming*, *Laughter*, *Wail*, *Moan*, *Groan*, *Narration*, *Monologue*, *Child speech*, *Kid Speaking*, and *Clapping*.

As noted earlier, YAMNet processes audio in fixed 0.48-second frames and outputs class probability estimates for each frame across all 521 audio event classes. To derive interaction cues, we aggregated predictions from two

¹Definitions of the 12 selected cues are available at <https://research.google.com/audioset/ontology/index.html>

consecutive frames (approximately one second), aligning with our foreground speech detection (FSD) design, which also operates at the two-frame level (Section 3.2). Using a one-second aggregation window enables the capture of fine-grained and transient interaction cues that reflect natural interaction dynamics, where airtime varies and paralinguistic behaviors—and periods of silence—may occur.

In contrast, assigning a single label to an entire 15-second window may obscure the presence of short but meaningful interaction cues within that interval. Accordingly, we computed the mean predicted probability across the two frames and selected the class with the highest averaged probability among all 521 classes as the final label. If this label belonged to our predefined set of 12 interaction cues, the instance was counted as containing an interaction cue.

3.4 Social Interaction Detection Pipeline

3.4.1 Recording Window and Duty Cycle. We recorded approximately 16 seconds of audio per sensing cycle, consisting of a 15-second intended recording window and an additional 1 second of padding to accommodate minor variability in actual recording duration (e.g., delays in microphone initialization). Such variability may arise from initialization overhead in the Health Sensor SDK and microphone, asynchronous invocation of event-driven sensor callbacks, sequential termination of other sensors prior to audio shutdown, and UI-thread latency. The additional padding increased the likelihood of obtaining at least 15 seconds of usable audio per cycle. For simplicity, we refer to this as a 15-second recording window throughout the remainder of the paper.

Audio sensing was performed using a 1.5-minute duty cycle, in which 15 seconds of audio were recorded followed by a 1 minute and 15 seconds gap with no audio capture. The choice of recording window and duty cycle was informed by prior work on conversational interaction patterns. Conversational turns are typically short, with a mean turn duration of approximately around 2 seconds [37], and gaps between turns are often very brief, on the order of 200 ms [36]. Based on these dynamics, we required interaction cues to be present in at least 50% of each 15-second window. This threshold reflects the intuition that, given rapid turn-taking and short response gaps, interaction-related cues are likely to occur in a substantial fraction of windows during an ongoing interaction.

Because dyadic interactions are the most common form of daily social interaction [57], it is reasonable to expect foreground speech to occur within at least some portion of a 15-second recording window during an ongoing interaction. At the same time, as discussed in Section 3.1, airtime varies substantially and individual speaking turns may extend beyond two minutes in certain settings [51, 66]. Accordingly, we did not impose a requirement that foreground speech be present in every 15-second window. Overall, the selected 1.5-minute duty cycle represents a practical balance between privacy preservation, resource consumption, and interaction detection accuracy, particularly given that prior work reports average interaction durations substantially longer than our sampling interval (e.g., approximately 5 minutes [62], and 13.97 or 20.19 minutes depending on tie strength [48]).

Our chosen duty cycle is shorter than those used in several prior systems, including the 12-minute sampling interval in the Electronically Activated Recorder (EAR) [46], the 3-minute interval used in AWARE [18], and continuous audio recording employed in recent smartwatch-based systems [39]. One motivation for adopting a shorter duty cycle was to better capture short interactions while simultaneously improving privacy and minimizing resource consumption. For example, if a 3-minute interval similar to AWARE had been used, our system would have missed 537 interactions shorter than 3 minutes that were successfully detected during real-world deployments (Section 5.4).

Finally, the short recording duration itself was intentionally selected to further enhance user privacy and reduce resource consumption. In comparison, the AWARE framework records 1 minute of audio per cycle [18], and EAR records 30 or 50 seconds of audio [50], whereas some recent systems rely on continuous recording [39].

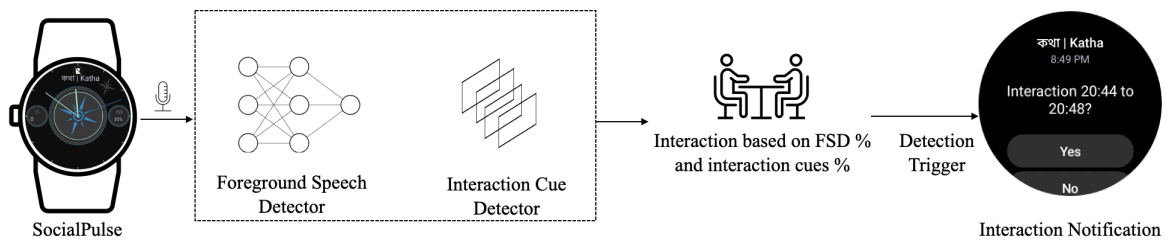


Fig. 3. On-watch SocialPulse pipeline for automatic social interaction detection.

By contrast, our approach limits both the duration and frequency of audio capture while retaining sufficient temporal resolution for reliable interaction detection.

3.4.2 Temporal Inference Procedure for Social Interaction Detection. Each 15-second audio recording is divided into non-overlapping 1-second windows for inference. This design choice is motivated by several considerations. First, the dataset used to train the FSD provides labels at a 1-second resolution, enabling more reliable predictions when inference is performed at the same temporal granularity. Second, shorter windows reduce the likelihood of overlapping speech between the watch wearer and others within a single segment. Prior work shows that when audio is segmented into 1-second windows, mixed speech occurs only 3% of the time in a 31-hour dataset [38]. In contrast, longer windows (e.g., 5 seconds) are more likely to contain overlapping speech, as conversational turns last around 2 seconds on average [37].

Similarly, interaction cues are unlikely to change at a sub-second timescale. Dividing audio into 1-second windows therefore preserves fine-grained paralinguistic cues while minimizing overlap, as emotional states typically do not fluctuate dramatically within such short intervals [4].

To reduce on-device computation, we do not apply FSD to all embeddings. Instead, we first identify embeddings corresponding to interaction cues and apply the FSD only to those candidate segments, improving resource efficiency while preserving detection accuracy.

An interaction is detected when two conditions are satisfied: (1) interaction cues are present at each probe start time, and (2) the proportion of foreground speech across the full interaction exceeds a predefined minimum threshold. For example, if a probe starting at 3:20:00 records a 15-second segment (3:20:00–3:20:15) in which at least 50% of the 1-second windows contain interaction cues, the system marks a potential interaction onset. If subsequent probes at 3:21:30–3:21:45 and 3:23:00–3:23:15 also satisfy this condition, the interaction is considered ongoing. If a later probe, for example, at 3:26:00–3:26:15 contains no interaction cues, the system marks the end of the interaction. To confirm that a genuine interaction occurred, the system verifies that at least 15% foreground speech is present. If this criterion is met, the interaction is labeled as occurring from 3:20:00 to 3:24:45, corresponding to the last probe with detected interaction cues. The full detection procedure is detailed in Algorithm 1 in the Supplementary Material.

We also account for exceptional cases to maintain interaction quality. For example, if a participant removes the smartwatch during an ongoing interaction, as detected by the off-body sensor, the system sets the interaction end time to the end of the last available recording. In such cases, evidence supports interaction continuity up to that point, but no further audio data are available to extend the detection.

4 On-Device Implementation of the Social Interaction Detection System

This section describes the on-device implementation of our interaction detection system, focusing on software architecture, model deployment, and runtime considerations for smartwatch-based inference. We primarily used Java for system development, including sensor control, data collection, and temporary on-device storage prior

to upload to Amazon S3. Python was used for model execution, contextual data handling, and audio feature extraction since it provides a richer ecosystem and supports future system extensions across a wide range of applications. To enable interoperability between Java and Python on the smartwatch, we employed the Chaquopy Python SDK².

For on-device model inference, we used TensorFlow Lite, which supports low-latency execution on resource-constrained devices. To ensure compatibility with the Python environment supported by Chaquopy, we aligned library versions used during model development with those available on-device. For example, we used scikit-learn version 1.1.3 and NumPy version 1.21.4, which were the latest supported versions in Chaquopy at the start of system development in 2024.

4.1 Sensor Configuration and Data Collection

Audio was recorded at a sampling rate of 16 kHz, which balances audio quality and power consumption relative to higher sampling rates (e.g., 44.1 kHz). Audio was initially captured in PCM format and converted to WAV format for processing using FFmpegKit³. This design enabled efficient buffering of audio data in memory, allowing the system to access the most recent 15-second segment without re-recording. This capability was necessary, for example, to determine whether a participant forgot to stop a manual recording after initiating it. Without buffering, the system would have required additional recording to recover the preceding audio segment, increasing resource usage.

In addition to audio, we collected heart rate, photoplethysmography (PPG), ambient light, step count, battery status, accelerometer, and gravity sensor data. As described in Section 3.4, we used the same data collection window across modalities, configuring a 16-second sensing interval with an intended duration of 15 seconds. For clarity, we refer to this window as 15 seconds throughout the paper, with the understanding that it corresponds to approximately 16 seconds of data.

Among these sensors, PPG data were collected via the Samsung Health Sensor SDK⁴. PPG was sampled continuously using batched delivery, in which samples are buffered and delivered in batches rather than triggering CPU wake-ups for each event. The CPU is activated when a batch is ready, resulting in substantial power savings [12].

All other sensors were sampled using a 1.5-minute duty cycle, consistent with the audio sensing configuration. For these sensors—except heart rate, which was collected at the fastest possible rate permitted by the hardware—we set the maximum reporting latency to 200,000 microseconds [14]. This choice was motivated by two factors. First, requesting the fastest possible reporting rate (0 microsecond) for all sensors would substantially increase battery consumption. Second, it helps control on-device storage usage. Given that the system stores audio log-mel spectrograms (computed with a 25 ms window and 10 ms hop), collects PPG continuously at 25 Hz, and may operate for multiple days between participant uploads, aggressive sensor reporting could rapidly exhaust on-device memory and lead to data loss once storage capacity is reached.

At the end of each data collection window, sensing was explicitly terminated within the sensor event listeners to improve resource efficiency. Scheduling alarms to stop sensors at predetermined times can introduce additional battery overhead [13]. Because multiple sensors were active and PPG data were sampled at 25 Hz, sensor callbacks were invoked frequently during each 15-second window, enabling timely termination of sensing without incurring additional scheduling overhead.

²<https://chaquo.com/chaquopy/>

³<https://github.com/arthenica/ffmpeg-kit>

⁴<https://developer.samsung.com/health/sensor/overview.html>

4.2 Participant Annotation of Social Interactions

To obtain reliable ground truth for naturally occurring social interactions while minimizing participant burden, we designed a smartwatch-based annotation workflow that combines automatic detection, participant feedback, and manual reporting. Because ecological momentary assessments (EMAs) were deployed on a smartwatch with a limited screen size, all annotation questions were phrased as concisely as possible, as illustrated in Figures 4 and 5. To minimize participant burden and avoid sleep disruption, notifications were suppressed during nighttime hours (12:00 AM–7:59 AM), even if participants wore the watch and potential interactions were detected.

Notifications served as the primary mechanism for collecting labels for detected interactions and related contextual information. When a notification was issued, the watch generated a 200 ms vibration to increase the likelihood that participants noticed the prompt.

Participants provided interaction annotations in three ways, all of which were used as ground truth: (1) responding to notifications associated with automatically detected interactions, (2) manually initiating and recording an interaction, and (3) responding to periodic prompts asking whether the system missed any interactions. Participants could respond directly to notifications on the watch or through the companion app.

To account for cases in which notifications were accidentally dismissed or cleared due to watch restarts, we retained access to recent notifications within the app. From the app interface, participants could navigate to previously issued prompts (e.g., missed interaction notifications) by selecting the corresponding option.

4.2.1 Participant Feedback on Auto-Detected Social Interactions. Within at most two minutes after an interaction ended, the system issued a notification (Figure 4) asking participants whether an interaction had occurred within a given time window. Participants could respond *Yes*, *No*, or *Maybe*. The *Maybe* option was included to account for cases in which participants were uncertain or had difficulty recalling details when responding after a delay.

Depending on the initial response, participants were presented with follow-up questions. If the response was *Yes* or *Maybe*, participants reported the number of people involved, the interaction mode (e.g., in-person or virtual), and an interaction rating. An additional “?” option was provided for both the number of people involved and the interaction rating to accommodate cases in which participants could not report these values precisely. If the response was *No*, participants indicated whether the detected start or end time was incorrect or whether no interaction had occurred. In such cases, participants also reported whether device-generated speech was present and whether people nearby were talking, enabling us to better understand potential sources of system errors in real-world settings.

Importantly, participants answered the same number of follow-up questions regardless of their initial response (*Yes*, *No*, or *Maybe*). This design choice was intended to reduce response bias, as requiring fewer questions for a particular option could incentivize its selection, particularly during busy or cognitively demanding moments.

4.2.2 Manual Reporting of Missed Social Interactions. Participants periodically received a notification asking whether the system had missed any interactions for which no automatic notification had been delivered (Figure 5(b)). The system was configured to prompt approximately every 80 minutes, with an added random delay of 0–5 minutes to avoid potential bias associated with fixed prompting intervals.

For resource efficiency, prompts were triggered at probe start times rather than via a separate scheduler. As a result, notifications could be delayed by up to one additional duty cycle (1.5 minutes), yielding an effective prompting interval of approximately 90 minutes. The notification asked: “Missed interaction [Start time] to [End time]?”

If participants responded *Yes*, they were instructed to add all applicable missed interactions by specifying their corresponding approximate start and end times. Throughout the paper, we refer to these manually reported events as *added interactions*.

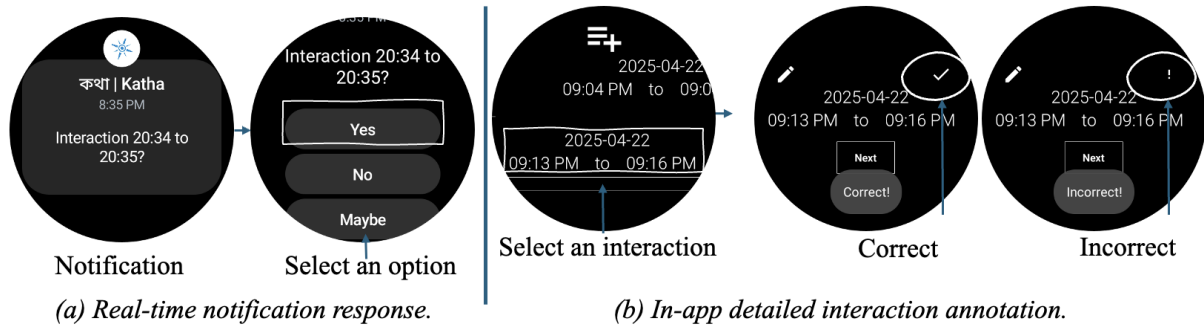


Fig. 4. SocialPulse feedback mechanisms for automatically detected social interactions: (a) real-time notification for marking whether interaction occurred and (b) a more detailed interface for annotating interactions.

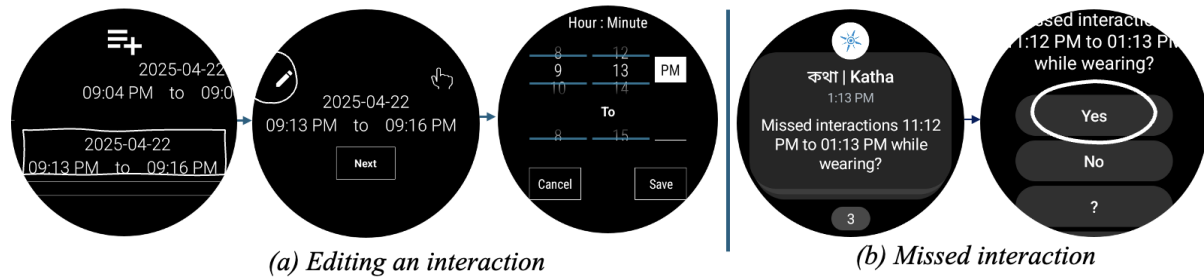


Fig. 5. Two features of SocialPulse: (a) editing a detected interaction and (b) responding to notifications about missed interactions.

4.2.3 Manual Recording of Social Interaction. Participants were instructed to manually record interactions when needed, particularly during virtual interactions, where acoustic data may be unavailable (e.g., when participants wear headphones). Manual recording could be initiated and terminated by pressing a button in the watch-based application.

Because participants might forget to press the *Stop* button after initiating a manual recording, the system included an automatic termination safeguard. Specifically, the system examined the most recent 15 seconds of buffered data and evaluated whether at least 50% of the 1-second windows contained interaction cues. If this minimum threshold was not met, the system automatically stopped the manual recording, marking the end of the interaction.

After manual recording ended—either through participant input or automatic termination—participants were prompted to answer the same set of follow-up questions used for automatically detected interactions. This ensured consistency in annotation across manual and system-detected interaction records.

4.3 Privacy-Preserving System Design

Our on-device system was designed with multiple safeguards to protect participant privacy throughout data collection, processing, and storage.

First, all data were collected with informed consent. The consent process explicitly described the study objectives, the sensors used, and the nature of the collected data. Participants were given opportunities to ask questions and could withdraw from the study at any time without penalty.

Second, sensing was automatically disabled whenever the smartwatch was removed from the participant's wrist. In addition, data were collected only in short recording windows of approximately 15 seconds, spaced at fixed intervals of 1 minute and 30 seconds. This duty-cycled design reduces continuous exposure while still supporting meaningful behavioral and health assessments. As discussed in Section 3.4.1, this recording duration is shorter than those used in several prior systems. To further promote transparency, our system displayed a visible "Recording..." indicator during each 15-second window.

Third, all data processing was performed on-device. Raw audio was stored only transiently and was deleted immediately after conversion into numerical representations, a process that typically completed within a few seconds. These intermediate numerical values were also discarded as soon as feature extraction and prediction were completed. Only a single derived audio representation—the log-mel spectrogram—was retained for downstream processing. This representation is more privacy preserving than raw audio and is widely used in audio analysis research [56].

Fourth, collected data were stored temporarily within the application sandbox, preventing access by other applications on the device. Processed data were then securely uploaded to Amazon S3, which provides both client-side and server-side encryption by default. Access to stored data was restricted to authorized members of the research team.

To further improve robustness while protecting sensitive annotations, interaction events and other sparse data (e.g., participant annotations and missed-interaction reports) were stored separately from high-sampling-rate physiological and behavioral sensing streams. Because interaction-level data are comparatively sparse and critical for model development, this separation reduces the risk that corruption or loss in high-volume sensor data will affect ground-truth labels. All retained data were stored in compressed formats and uploaded securely, supporting reliable long-term deployment under resource and privacy constraints.

Finally, all privacy and security measures were reviewed and approved by the university's Institutional Review Board (IRB) and IT security office, ensuring compliance with institutional and ethical standards for human-subject research.

4.4 Pre-Deployment System Testing

Before the main deployment, we conducted pre-deployment testing with 11 participants to assess real-world system behavior and identify major usability or reliability issues. Participants wore the smartwatch for several days (38 participant-days total), during which the system automatically detected 343 interactions; 73.18% ($N = 251$) were confirmed as correct by participants. Follow-up discussions with six participants indicated high recall: participants did not report any interactions lasting at least two minutes that they believed occurred without a corresponding notification. Participants also reported that frequent notifications could be burdensome on socially dense days. Based on this feedback, we refined the study protocol for the main deployment by limiting participation to three days and capping interaction-related notifications at a maximum of four per hour to balance annotation quality with participant burden.

5 In-the-Wild Deployment and Evaluation

Following pre-deployment testing and system refinement, we conducted a real-world deployment to evaluate the system's performance, usability, and robustness in everyday settings.

5.1 Participants

We recruited $N = 38$ participants from a large public university in the southeastern United States, including undergraduate students ($n = 13$), graduate students, staff, and faculty members ($n = 25$). All study procedures were approved by the university's IRB and were conducted under the supervision of a licensed clinical psychologist

and members of the research team. To avoid potential bias, research assistants affiliated with the laboratories conducting the study were not eligible to participate.

The sample was predominantly composed of heterosexual Asian and White non-Latinx women, with a mean age of 25.42 years ($SD = 8.19$). Participant demographic characteristics are summarized in Table 2.

Table 2. Demographic characteristics of participants in our study on 38 participants.

Characteristic		<i>n</i>	%
Gender	Woman	20	52.63
	Man	17	44.74
	Non-Binary	1	2.63
Race	Caucasian/White	14	36.84
	Asian	17	44.74
	Multiple Races	4	10.53
	African American	2	5.26
	Middle Eastern	1	2.63
First Language	English	25	65.79
	Not English (e.g., Bengali, Chinese, Indonesian, Kannada)	13	34.21

5.2 Study Design and Participant Protocol

Participants were recruited through two channels: (1) a university research participation pool for paid research studies and (2) targeted advertisements distributed via email lists within specific schools, departments and research labs.

After enrollment, participants completed an initial study visit that included informed consent and hands-on instruction in using the smartwatch-based system (e.g., uploading data and responding to ecological momentary assessments). Participants were provided with a detailed user manual during the visit and received an electronic copy by email afterward. Study visits were conducted by trained research staff and undergraduate research assistants affiliated with a psychology laboratory. All study personnel received training in human subjects research, informed consent procedures, study background and protocols, and use of the smartwatch system to ensure consistent and accurate participant onboarding.

Each participant was instructed to wear the smartwatch for three consecutive days, including two weekdays and one weekend day (either Thursday–Saturday or Sunday–Tuesday). This schedule was designed to capture variability in social interactions across structured weekdays and less-structured weekends. Participants were not permitted to select their own study days to reduce selection bias (e.g., choosing days with minimal social activity). Participants were encouraged to wear the watch during their active hours to maximize the likelihood of capturing social interactions.

Researchers monitored participant compliance with smartwatch wear and EMA completion throughout the study. Participants also received reminder emails as needed (e.g., prompts to wear the watch or complete EMA responses). Participants could earn up to \$50 in compensation, with payment determined by participation rate, calculated as the product of smartwatch wear duration and the proportion of EMA prompts completed within two hours.

This project was automatically issued a National Institutes of Health (NIH) Certificate of Confidentiality upon grant award. All study data were de-identified prior to analysis and sharing in accordance with funder guidelines and open science best practices.

5.3 Data Quality and Sensor Coverage

Across the deployment, participants wore the smartwatch for a total of 120 days, with an average usage duration of 3.16 days per participant ($SD = 0.64$). Participants were instructed to wear the smartwatch for three consecutive days; however, some participants wore the device for longer periods. In such cases, we included up to four days of data. This inclusion was consistent with our approved IRB protocol, as it did not alter the human-subjects design and participants were compensated accordingly. For simplicity, we refer to the study duration as three days throughout the paper, reflecting the average usage of 3.16 days.

For model development, we excluded heart rate, step count, and battery sensors. Instead of heart rate, we relied on photoplethysmography (PPG) data sampled at approximately 25 Hz, which provides substantially higher temporal resolution than heart rate measurements configured at approximately 1 Hz (the maximum supported rate without relying on specialized SDKs). PPG captures beat-to-beat interval dynamics and thus offers richer physiological information than heart rate expressed in beats per minute. Step count and battery level were recorded once per probe start to improve resource efficiency, given the limited variability expected within a 15-second sensing window. Due to the resulting low sample counts, these signals were not included in subsequent analyses.

As shown in Figure 6(b), for the sensors used in multimodal model development (Section 6)—including Audio, PPG, Accelerometer, Gravity, and Light—the number of collected samples was largely consistent across the study period, with greater variability observed for the accelerometer and gravity sensors. Despite this variability, when data were present, observed sample counts were often higher than the nominal sampling rates.

One plausible explanation for these elevated sampling rates is the Android-based Wear OS sensor architecture, in which multiple applications communicate with the Android sensor framework and share a single-client sensor hardware abstraction layer (HAL) [15]. When different applications request the same sensor at different sampling rates (e.g., one at 10 Hz and another at 20 Hz), the sensor delivers data at the highest requested rate. As a result, applications requesting lower rates may still receive data at higher frequencies [15]. Consequently, sensing data cannot be guaranteed to arrive at a perfectly constant sampling rate.

During the deployment period, all sensors—including Audio, PPG, Accelerometer, Light, Heart Rate, Step, and Battery—were activated more than 37,000 times for data collection, closely matching the expected number of sensor activations (Figure 6(a)), with the exception of the gravity sensor.

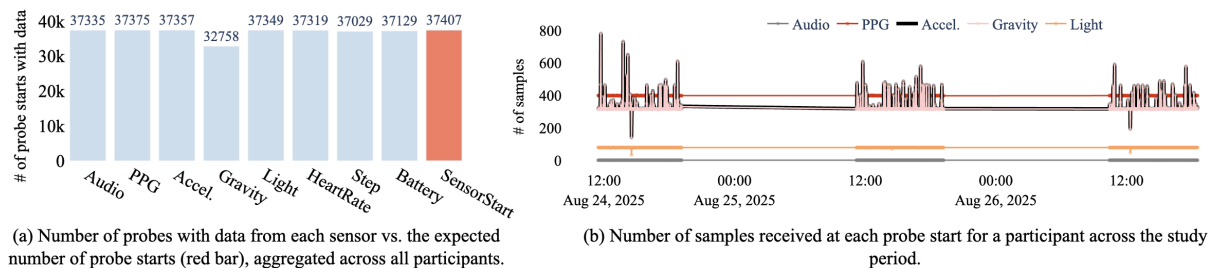


Fig. 6. Sensing data quality of the on-device system in real-world deployment. (a) Sensor activation counts across participants and days. (b) Sample counts for sensors used in multimodal analysis. Heart rate, step, and battery sensors are excluded for clarity. The accelerometer line width is increased to distinguish it from the gravity sensor, which has a similar sampling rate.

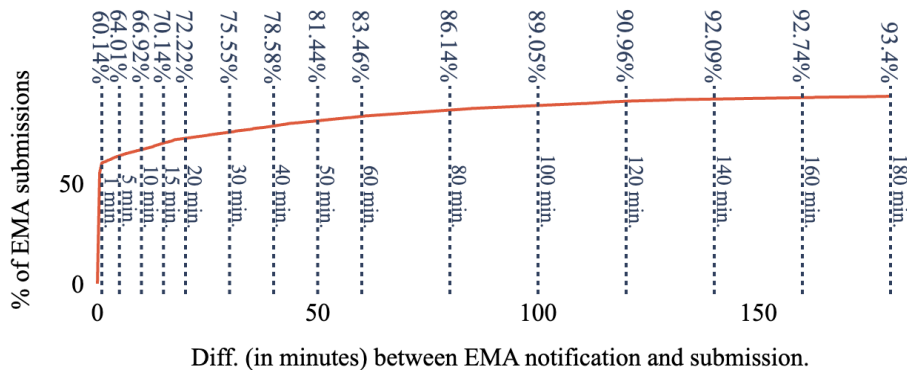


Fig. 7. Difference (in minutes) between system notification time and participant EMA submission time. For readability, the figure includes only EMAs submitted within 3 hours of notification ($N = 1,570$, 93.4%).

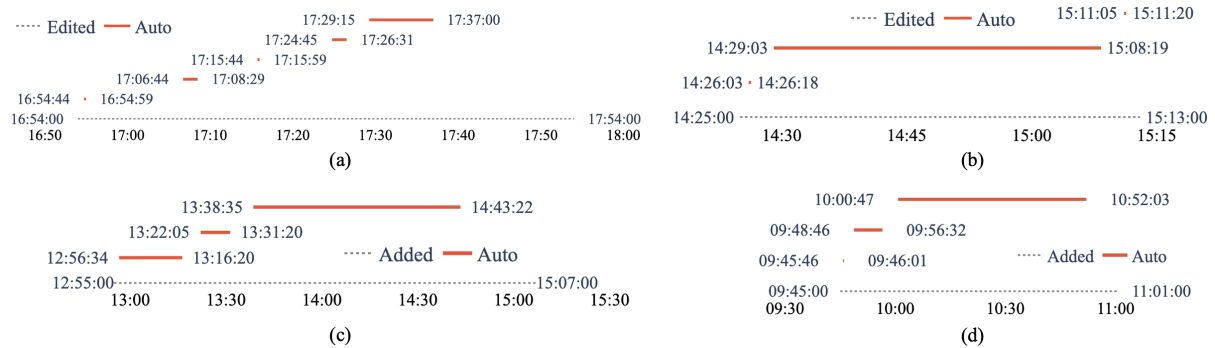


Fig. 8. (a–b) Examples of participant-edited interaction start and end times, with the system’s automatically detected interactions occurring within the edited intervals. (c–d) Examples of participant-added interaction start and end times provided in response to notifications about potentially missed interactions, along with the system’s automatically detected interactions within the added intervals. The y-axis is used solely for visualization, with interaction segments stacked on parallel lanes using a constant vertical offset for readability.

5.4 In-the-Wild System Performance

5.4.1 EMA Response Latency. After preprocessing, 1,691 automatically detected interactions received participant responses. For each notification, participants indicated whether the detected interaction was correct, incorrect, or a *maybe* interaction, followed by a set of context-specific follow-up questions (Section 4.2).

Among these 1,691 interactions, participants responded to 60.14% of notifications within 1 minute and 75.55% within 30 minutes (Figure 7). Notably, 90.96% of notifications were answered within 2 hours, indicating strong responsiveness and supporting the reliability of participant-provided annotations.

5.4.2 Missed and Participant-Edited Interactions. In total, participants responded to 510 notifications querying whether the system had missed any interactions. On average, each notification covered an 82.74-minute window ($SD = 1.59$), excluding 44 notifications (8.62%) that exceeded 90 minutes. These longer windows likely occurred when participants did not wear the watch for extended periods following the previous missed-interaction

prompt. Because the system automatically disables sensing when the watch is removed to protect privacy, missed-interaction notifications could not be issued in a timely manner in these cases.

Across the 510 notifications, participants reported no missed interactions in 79.8% of cases ($N = 407$). These notifications spanned a cumulative duration of 584.35 hours during which participants indicated that no interactions were missed. In contrast, participants reported missed interactions in 17.06% of cases ($N = 87$). For these cases, participants provided start and end times for the missed interaction.

To assess whether the auto-detector identified interactions during these added-interaction intervals, we compared the reported intervals with auto-detected interaction segments using two overlap criteria: (1) whether the start or end of any auto-detected interaction fell within an added-interaction interval, and (2) whether the start or end of an added-interaction interval fell within an auto-detected interaction segment. Using these criteria, we found that 63.54% of added interactions overlapped with auto-detected interactions (e.g., Figure 8(c, d)).

Among the added interactions, 18.75% were reported as virtual interactions, and 10.42% had durations shorter than the 1.5-minute duty cycle. Both conditions can hinder reliable detection, as the system relies on intermittent acoustic sensing. Additionally, for 22.91% of added interactions, the number of probe start times within the reported interval was lower than expected, suggesting that the watch may not have been worn continuously or may have been removed during these interactions. This reduction can also be attributed to Wear OS not triggering background tasks at perfectly regular intervals, particularly under low-power idle modes [13].

Participants also edited 123 auto-detected interactions. In 74.8% of these cases, the edited interactions showed no change from the automatically detected start and end times. One plausible explanation is accidental button presses on the smartwatch's small screen, such as when participants intended to select a different function. Participants may also have entered the edit interface to explore the application without making changes. For the remaining edited interactions, although the edited timestamps did not exactly match the automatically detected intervals, some auto-detected interactions were fully contained within the edited ranges (Figure 8(a, b)).

Within the time windows of edited and added interactions, there were 33 auto-detected interactions that participants explicitly marked as incorrect. A plausible explanation is that, although these detections occurred within participant-confirmed interaction periods, their durations were shorter than the corresponding edited or added interactions, leading participants to perceive them as incorrect. In our quantitative evaluation of real-world deployment (Section 5.4.3), we treated these 33 detections as correct, as they occurred within interaction intervals confirmed by participant-provided edits or additions.

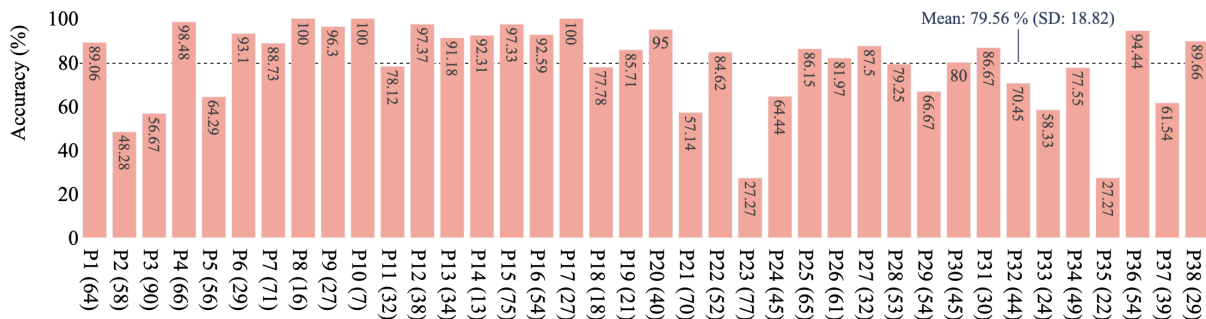


Fig. 9. Per-participant accuracy of the deployed auto-detection system. Values in parentheses indicate the total number of automatically detected interactions to which each participant responded. The dotted black line indicates the mean accuracy across all participants.

5.4.3 Performance of the Deployed System in the Wild. Among the 1,691 automatically detected interactions, ten were labeled as *maybe*, indicating participant uncertainty about whether an interaction occurred, consistent with the definition provided in the user manual. These ten cases were excluded from performance evaluation. Of the remaining interactions, 77.28% ($N = 1,299$) were confirmed as correct by participants.

Participant-level analysis showed a mean accuracy of 79.56% ($SD = 18.82\%$), with per-participant accuracy ranging from 27.27% to 100% (Figure 9). Notably, for 71.05% of participants, the system achieved an accuracy of at least 75%.

Analysis of correctly detected interactions indicated that interaction onsets occurred across hourly bins from 8:00 AM to 11:00 PM (Figure 10(a)). Interaction durations ranged from under 1 minute ($N = 322$, 24.79%) to over 1 hour ($N = 36$, 2.77%) (Figure 10(b)). All interaction modes were observed, including in-person ($N = 1,058$, 81.45%), virtual ($N = 204$, 15.70%), and hybrid ($N = 24$, 1.85%) interactions (Figure 10(c)). Most interactions involved two participants ($N = 802$, 61.74%), as reported by participants (Figure 10(d)).

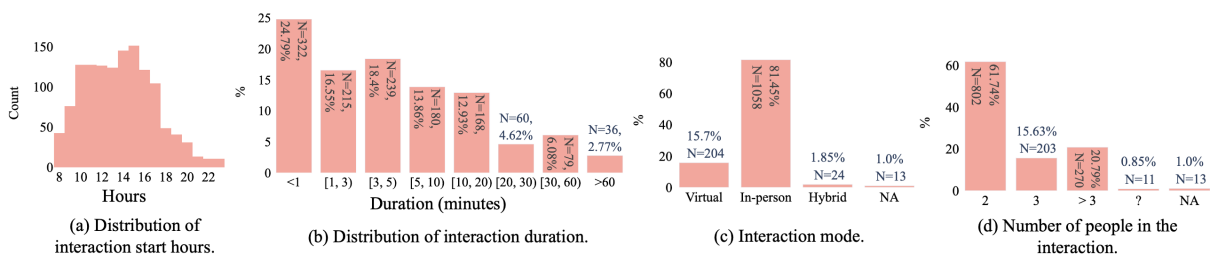


Fig. 10. Statistics on correctly auto-detected interactions in real-time by our on-watch system. NA: Not available. "?" denotes "Do not know."

5.4.4 Analysis of Social Interaction Detection Errors. To investigate sources of detection errors, participants reported whether speech from nearby devices (e.g., television) or nearby people was present during incorrectly detected interactions. Among incorrect detections, 64.66% ($N = 247$) involved speech from electronic devices, while 28.01% ($N = 107$) involved speech from nearby people, indicating that non-interaction speech remains a primary source of confusion in real-world settings.

To quantify differences between correct and incorrect detections, we analyzed the proportion of foreground speech within detected interactions. For most participants, foreground speech percentages were higher in correctly detected interactions than in incorrect ones. We compared per-participant mean foreground speech percentages using a Wilcoxon signed-rank test excluding three participants with 100% accuracy. Across the remaining 35 participants, the Wilcoxon test revealed a statistically significant difference ($p = 0.00009$), suggesting that participant-specific foreground speech thresholds—rather than the fixed 15% threshold used in the deployed system—may further reduce errors.

Despite this robustness, some errors persisted, particularly when speech-emitting devices or nearby conversations were in close proximity to the watch. The relatively low foreground speech threshold of 15% was intentionally selected to prioritize sensitivity and reduce missed interactions, supporting higher-quality annotation at the expense of some false positives. These findings highlight opportunities for adaptive or personalized thresholds in future systems.

5.4.5 On-Device Resource Consumption. Across 37,353 probe start events, the system recorded the time required to process audio, perform inference, and save outputs (Figure 12(a)). The mean processing time per probe was 13.286 seconds ($SD = 27.28$ seconds), while the median processing time was substantially lower at 3.183 seconds.

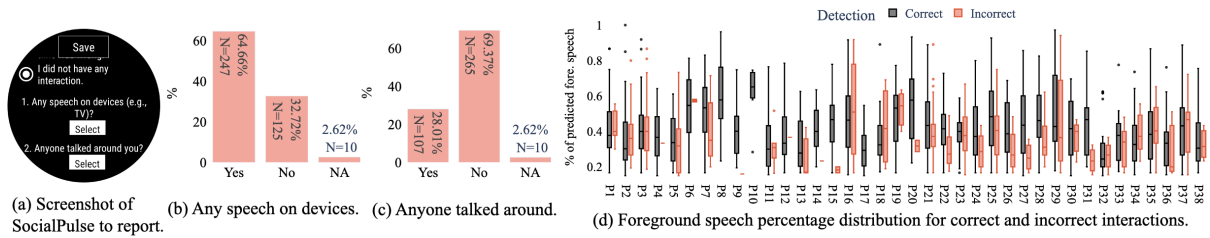


Fig. 11. (a) Screenshot of our reporting interface, when a participant marked an interaction as inaccurate. (b–c) Distributions of participant responses related to surrounding speech. (d) Distribution of predicted foreground speech percentages for correct and incorrect interactions. NA: Not Available.

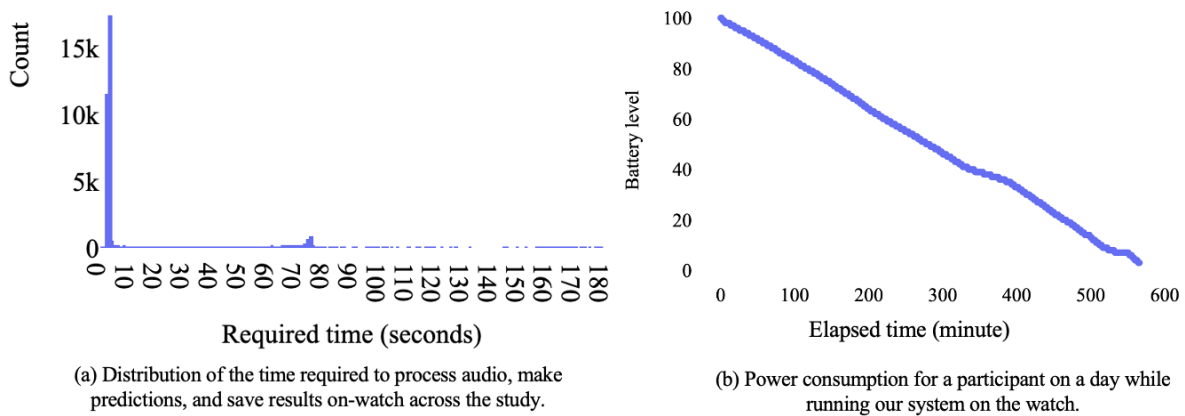


Fig. 12. On-watch resource consumption of the system. (a) Processing time per probe, computed from 37,353 processing-time logs collected across the study. For readability, only instances with processing times of at most 3 minutes are shown, accounting for 99.84% of all recorded probes.

In 77.87% of probe events, the total processing time was under 4 seconds, indicating that the majority of inference operations completed quickly despite occasional longer delays.

We also analyzed power consumption during deployment. For a representative participant, the cumulative system usage attributable to sensing and inference was approximately 600 minutes over the study period, as illustrated in Figure 12(b).

6 Multimodal Model for Social Interaction Detection

Building on the real-world deployment and participant-provided annotations, we next developed a multimodal model to identify social interactions using the collected wearable sensing data. This model leverages synchronized signals across modalities to capture interaction dynamics beyond any single sensor stream.

6.1 Labeling Strategy for Multimodal Model Training

To train the multimodal interaction detection model, we assigned labels to each 15-second data collection window based on participant-confirmed interaction annotations (Figure 13). Windows whose timestamps fell within participant-labeled interaction intervals were labeled as class 1 (presence of social interaction). Windows outside

these intervals were treated as candidates for class 0 (no interaction), subject to conservative filtering described below.

Results from the deployed interaction detection system and participant responses to missed-interaction notifications indicate high recall (Section 5.4.2). That is, when an interaction occurred, the system was highly likely to notify the participant. This observation motivated us to include windows with no detected interactions as class 0, provided there was sufficient evidence that no interaction occurred during those intervals.

Reliable ground-truth labels were unavailable for automatically detected interaction intervals when participants did not respond to notifications. To preserve labeling accuracy, we excluded all windows associated with such unresponded detections from model training.

Because raw audio was not stored for privacy, we reconstructed the deployed interaction detection pipeline offline using the on-device–saved log-mel spectrogram features. This reconstruction enabled us to identify excluded interaction intervals and verify labeling consistency without requiring access to raw audio. We confirmed that reconstructed interaction boundaries aligned with those produced by the deployed system within the 15-second sensing resolution used for labeling.

To further reduce the risk of mislabeling non-interaction windows, we applied conservative filtering informed by exploratory analysis of foreground speech. Specifically, we excluded candidate interaction windows with ambiguous foreground speech levels, retaining only windows with clear evidence of interaction or non-interaction. Given that such ambiguous cases were rare and labeling was performed at a 15-second resolution, we do not expect these exclusions to affect model performance or generalization.

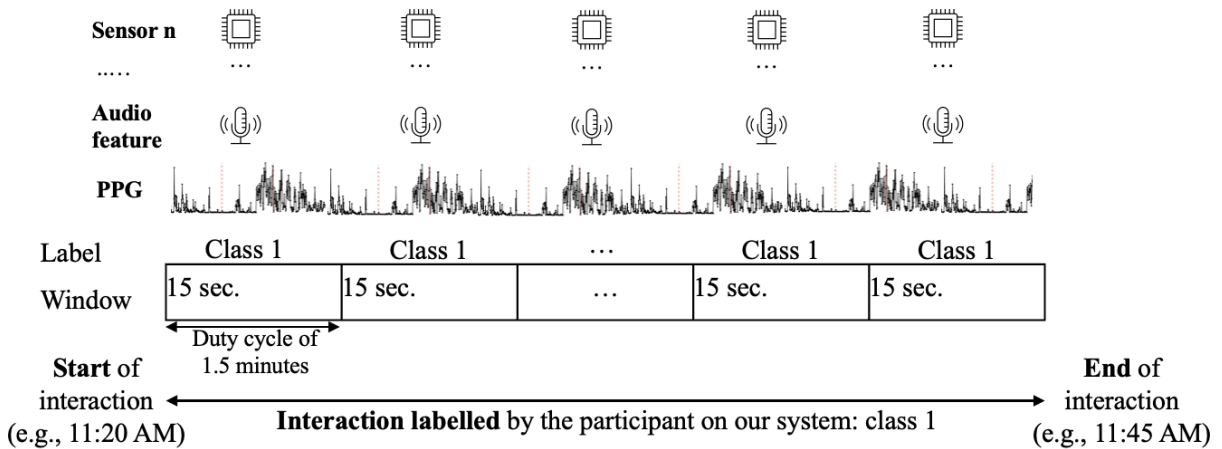


Fig. 13. Labeling was performed on the 15-second data segments collected in each duty cycle. While PPG data were collected continuously (as illustrated in the figure), all other sensors recorded data for 15 seconds every 1.5 minutes.

6.2 Multimodal Model Design and Training

We developed a convolutional neural network (CNN)–based multimodal model to identify social interactions from wearable sensing data. CNNs are well suited for capturing complex patterns in structured representations and are more parameter-efficient than fully connected networks due to weight sharing and partial connectivity [23]. Because each probe captured only 15 seconds of data, the number of raw samples per modality was limited (e.g., approximately 90 accelerometer samples per probe). Such short time-domain signals are often insufficient for

training deep learning models directly. We therefore transformed all raw sensor signals into spectrogram-based representations.

Sampling Rate Normalization. During preprocessing, we observed variability in the number of samples collected per probe window. For example, across approximately 8,000 probes, accelerometer data were received at 19.9375 Hz, substantially higher than the most common sampling rate of 6.25 Hz. As discussed in Section 5.3, this behavior is expected due to Android’s sensor sampling framework.

However, variable temporal resolutions across probe windows can introduce inconsistency when training CNNs, as convolutional filters may extract non-comparable features from inputs with different sampling structures. To ensure consistent representations across all probe windows, we resampled each sensor stream to a fixed sampling rate per modality. For each sensor, we selected the most frequently observed sampling rate and rounded minor variations. For example, accelerometer sampling rates of 6.125 Hz, 6.25 Hz, and 6.3125 Hz were treated as 6 Hz and resampled accordingly. When a probe window contained more samples than required, we applied averaging; when samples were missing, we used interpolation. Each probe window was processed independently to avoid information leakage and to reflect real-world inference conditions.

An exception was made for the gravity sensor. Although its most frequent sampling rate was 19.8125 Hz, the second most frequent rate was 6.25 Hz. Using the higher rate would have required extensive interpolation for more than 5,000 probe windows sampled at approximately 6 Hz, potentially distorting the signal. We therefore adopted a 6 Hz sampling rate for the gravity sensor to minimize missing data and better preserve real-world signal characteristics.

Feature Construction. For accelerometer and gravity signals, we computed the magnitude across the three axes. Photoplethysmography (PPG) signals were preprocessed using NeuroKit2 [47], and spectrograms were generated from the cleaned waveforms. To balance time and frequency resolution given the limited data per probe, we used a segment length of 16 samples, an FFT size of 16, and an overlap of 12 samples. Based on the resulting sample counts, spectrogram images of size 112×112 were used. During preliminary experiments, smaller images consistently outperformed larger ones (e.g., 112×112 vs. 224×224), likely because compact representations better preserve informative structure given the limited signal length. All reported results use 112×112 images.

Model Architecture. The multimodal architecture is shown in Figure 14. Each modality was processed by a convolutional layer followed by batch normalization and ReLU activation, then three residual blocks [24]. Skip connections in the blocks facilitate optimization and improve representational learning [23]. We used He initialization, consistent with ResNet-style architectures. We did not adopt a full ResNet model due to its large parameter count (e.g., ~11.7 million parameters for ResNet-18), which is impractical for real-time on-watch inference.

After the residual blocks, we applied global average pooling (GAP) to each modality-specific branch. The resulting feature vectors were concatenated to form a fused multimodal representation, followed by two fully connected layers with 64 and 32 neurons (ReLU activation). A final sigmoid-activated output layer produced the probability of social interaction.

To reduce overfitting, we applied on-the-fly data augmentation during training, including temporal flipping, slight temporal stretching (scale=1.001–1.05) followed by cropping to 112×112 , and additive Gaussian noise (mean=0, SD=0.05). Stretching was applied along the temporal axis to preserve meaningful temporal dynamics in the spectrograms.

Training Procedure. Because social interactions are less frequent than non-interaction periods, we used weighted binary focal loss to address class imbalance. The model was optimized using stochastic gradient descent with a learning rate of 0.05, batch size of 32, and up to 50 epochs. Early stopping was applied based on validation loss,

terminating training if the loss did not decrease for five consecutive epochs. Training data were shuffled prior to learning to avoid ordering artifacts.

Cross-Validation Strategy. We evaluated the model using a Leave-One-Participant-Out Cross-Validation (LOPOCV) scheme. In each iteration, one participant was held out for testing. From the remaining $n - 1$ participants, two with the smallest class-count difference were selected for validation to reduce bias from extreme class imbalance. The remaining $n - 3$ participants were used for training.

Meta-Learning Integration. In a final meta-learning stage, we incorporated the percentage of interaction cues and the percentage of foreground speech as additional features, together with predicted probabilities of social interaction from two multimodal models (e.g., Accelerometer–Audio and Light–Audio). Foreground speech was estimated using the FSD (Section 3.2) only for frames containing interaction cues, consistent with the deployed system (section 3.4) and to reduce computational overhead. We evaluated the top-performing meta-learners from the FSD analysis—Logistic Regression, LinearSVC, and NearestCentroid—favoring these simple models for their generalization ability and reduced risk of overfitting.

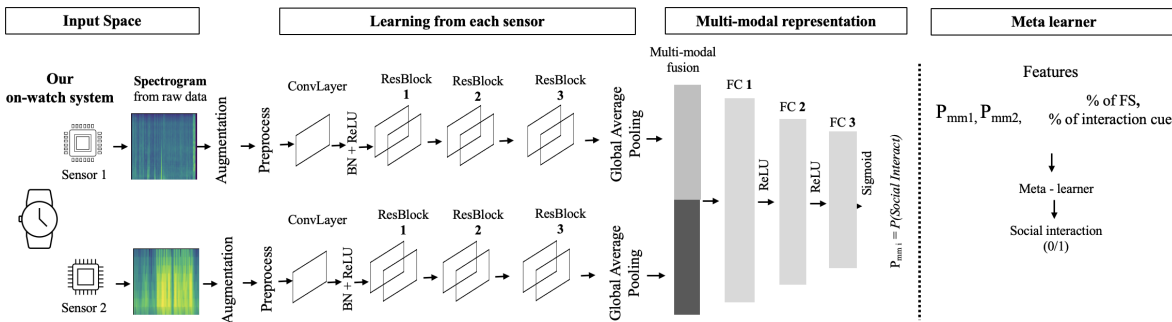


Fig. 14. Architecture of our multi-modal model. ConvLayer: Convolution layer, ResBlock: Residual block, FC: fully connected. P_{mm1} and P_{mm2} presents the probability to have an interaction based on multi-modal model 1 (e.g., Audio–Accelerometer) and multi-modal model 2 (e.g., Audio–PPG) respectively. FS: Foreground speech.

6.3 Model Evaluation and Baseline Models

To evaluate model performance, we report accuracy, precision, sensitivity, specificity, and F1 score. Precision and F1 score are computed using macro averaging, which assigns equal weight to each class. We additionally report balanced accuracy, defined as the average of sensitivity and specificity. Balanced accuracy and sensitivity are treated as the primary evaluation metrics, as they better capture performance under class imbalance, with sensitivity reflecting the model’s ability to correctly identify interaction windows.

As baseline models for interaction detection, we used MobileNetV1 [25] and YAMNet [58], two publicly available architectures that are widely used across mobile and audio-based prediction tasks. MobileNetV1 contains approximately 3.3 million parameters and is optimized for mobile and embedded devices. YAMNet is built on MobileNetV1 and pretrained on more than 2 million YouTube videos spanning 521 audio event classes (e.g., conversation), as described earlier. We adapted the baseline development procedures described in [39], which also evaluated these architectures for interaction-related tasks.

For YAMNet, we implemented the “YAMNet + FC” baseline from [39], in which three fully connected layers are trained on YAMNet embeddings. Specifically, embeddings were averaged across each 15-second window, and

the resulting vector was used as input to the fully connected classifier. For MobileNetV1, we trained the model from scratch, adapting the general approach described in [39].

When implementation details were not explicitly specified in [39], we followed standard practice. For example, the prior work does not describe how validation and test sets were separated during training. Therefore, consistent with prior studies using LOPOCV [31], we selected one participant for validation in each fold when training baseline models. The validation participant was randomly chosen in each iteration, as using the same participant for validation across all LOPOCV folds could introduce bias.

We could not implement the main architecture proposed by [39] as baselines for two practical reasons. First, we needed raw audio to generate spectrograms following their feature-extraction procedure. Second, their fusion design relies on constructing spectrograms from 30 consecutive 1-second sub-clips within each 30-second window; without raw audio, we could not generate spectrograms at this 1-second granularity. To protect participant privacy and collect real-world data, our system computed features on-device and saved only the log-mel spectrogram for the full 15-second probe window.

6.4 Performance of the Multimodal Model

Across all evaluated configurations, multimodal models that included the audio modality consistently outperformed models based solely on non-acoustic sensors (Table 3). The best-performing configuration combined accelerometer and audio data, achieving a balanced accuracy of 86.18%. Other audio-inclusive combinations—Gravity–Audio, Light–Audio, and PPG–Audio—also demonstrated strong performance, with balanced accuracies of 85.75%, 85.67%, and 85.65%, respectively.

In contrast, models relying exclusively on non-acoustic modalities performed substantially worse. For example, the PPG–Accelerometer configuration achieved a balanced accuracy of approximately 51%, close to chance level. These results highlight the importance of acoustic information for reliable social interaction detection, even when combined with rich physiological and inertial sensing data.

Sensors	N samples	Precision	Sensitivity	Specificity	BA	F1	Accuracy
Accelerometer_Audio	33700	83.97	85.36	87.00	86.18	84.86	86.49
Accelerometer_Gravity	29624	55.19	13.19	91.26	52.22	49.72	67.50
Accelerometer_Light	33709	59.48	9.87	95.33	52.60	48.49	68.43
Gravity_Audio	29621	83.25	84.80	86.71	85.75	84.25	86.13
Light_Audio	33704	83.47	84.68	86.65	85.67	84.35	86.03
Light_Gravity	29628	55.53	7.68	95.14	51.41	46.86	68.53
PPG_Accelerometer	33700	52.55	12.06	90.16	51.11	48.14	65.57
PPG_Audio	33683	83.30	85.06	86.25	85.65	84.23	85.87
PPG_Gravity	29613	54.31	14.86	89.41	52.13	50.13	66.72
PPG_Light	33694	49.95	6.18	93.80	49.99	44.75	66.21

Table 3. Performance of multimodal models without the meta-learner. Bold colored texts presents the best model in terms of balanced accuracy (BA). N samples presents the number of samples used for model evaluation.

After evaluating the multimodal models, we developed a meta-learner as defined in the multimodal architecture (Figure 14). The meta-learner integrates the predicted probabilities from two multimodal models along with two summary features computed for each data collection window: the percentage of foreground speech and the percentage of detected interaction cues.

Across different pairs of multimodal models, the meta-learner achieved comparable performance, with balanced accuracy consistently exceeding 90%, indicating robustness to the choice of input models. We report results using the Accelerometer–Audio and Light–Audio configurations, which correspond to the top-performing multimodal models (Table 3), excluding Gravity–Audio. Although the Gravity–Audio configuration achieved a slightly higher balanced accuracy than Light–Audio, the Light–Audio modality provided a substantially larger number of samples for evaluation, enabling more reliable performance estimates.

Using these modalities, the LinearSVC-based meta-learner achieved a sensitivity of 91.17%, a specificity of 89.56%, and a balanced accuracy of 90.36%, outperforming all baseline models.

Algorithm	N Samples	Precision	Recall	Specificity	BA	F1	Accuracy
Meta-learner (Logit)	33698	88.02	90.59	90.00	90.30	88.97	90.19
Meta-learner (NearestCentroid)	33698	88.18	90.38	90.27	90.33	89.09	90.31
Meta-learner (LinearSVC)	33698	87.86	91.17	89.56	90.36	88.88	90.07
Baseline 1 (MobileNetV1)	33698	82.93	71.18	91.07	81.13	81.92	84.81
Baseline 2 (YAMNet + FC)	33698	87.77	82.36	92.57	87.47	87.62	89.36

Table 4. Performance of different algorithms used to train our meta-learner. The meta-learners were trained with predicted probabilities of Accelerometer_Audio and Light_Audio based multi-modal models, along with percentage of foreground speech and interaction cues. The bold colored line shows the best model in terms of both balanced accuracy (BA) and sensitivity (recall).

6.5 Discussion

6.5.1 Ablation Study. To identify the contribution of individual sensors and model components, we conducted an ablation study. Specifically, we trained single-sensor models using the same architecture as the multimodal model, restricting the network to a single sensor branch (i.e., retaining only the residual blocks corresponding to one sensor in Figure 14 and removing all other modality-specific components).

Consistent with the multimodal results, the audio-only model substantially outperformed models based on other individual sensors. The audio-only configuration achieved a balanced accuracy of 86.41%, whereas the accelerometer-only model achieved a balanced accuracy of 49.44% (Table 5). This finding underscores the dominant role of acoustic information in distinguishing interaction from non-interaction in naturalistic settings.

Sensor	N samples	Precision	Sensitivity	Specificity	BA	F1	Accuracy
Accelerometer	33727	46.91	3.31	95.57	49.44	42.75	66.53
Audio	33858	84.53	84.85	87.98	86.41	85.33	87.00
Gravity	29639	51.06	8.37	92.35	50.36	46.39	66.80
Light	33721	53.27	5.11	96.13	50.62	44.60	67.48
PPG	33752	47.77	8.07	90.20	49.13	45.04	64.34

Table 5. Performance of model based on single sensor.

To further examine the contribution of individual architectural components, we conducted an ablation study by systematically removing components from the network, ranging from the ResNet-based preprocessor to the fully connected layers. When excluding the ResNet-based preprocessor, we applied standard feature scaling, as

neural networks typically require normalized inputs. Under this configuration, the Accelerometer–Audio model exhibited an approximately 1% reduction in both sensitivity and balanced accuracy. Given that the evaluation was performed on 33,700 samples, this performance decrease is non-trivial.

Similar degradations were observed when removing most other components. Although excluding the second fully connected layer resulted in a marginally higher balanced accuracy (86.31% vs. 86.18%) for the Accelerometer–Audio model, this change was accompanied by slight reductions in F1 score and precision. In contrast, for the audio-only model, removing the second fully connected layer led to an approximately 1% decrease in both balanced accuracy and sensitivity, highlighting the utility of this component for audio-based interaction detection.

Overall, these results suggest that while the proposed architecture is effective, certain components may be removed to reduce model complexity when parameter efficiency is prioritized, with only modest trade-offs in performance.

Config.	Accelerometer and Audio						Audio					
	N	Prec.	Sens.	Spec.	BA	F1	N	Prec.	Sens.	Spec.	BA	F1
e_aug	33700	83.02	84.36	86.19	85.28	83.92	33858	84.92	83.88	88.85	86.37	85.56
e_ResNetPro	33700	82.75	83.65	86.15	84.90	83.61	33858	82.85	82.68	86.74	84.71	83.63
e_Conv	33700	83.30	84.45	86.53	85.49	84.18	33858	84.08	85.93	86.93	86.43	85.02
e_1st_resB	33700	83.83	84.59	87.17	85.88	84.68	33858	83.01	83.12	86.76	84.94	83.81
e_mid_resB	33700	83.43	85.80	86.09	85.94	84.40	33858	83.18	85.11	86.08	85.60	84.12
e_last_resB	33700	83.37	84.27	86.70	85.48	84.23	33858	83.05	84.20	86.33	85.26	83.93
e_All3_resB	33700	74.91	76.30	78.52	77.41	75.66	33858	75.44	77.63	78.58	78.11	76.21
e_1st_Dense	33700	83.11	85.30	85.87	85.59	84.06	33858	84.00	85.50	87.01	86.26	84.91
e_2nd_Dense	33700	83.72	86.44	86.18	86.31	84.71	33858	83.08	85.19	85.91	85.55	84.04
e_bothDense	33700	83.78	82.35	88.04	85.20	84.41	33858	83.66	83.46	87.45	85.46	84.42
Whole arch.	33700	83.97	85.36	87.00	86.18	84.86	33858	84.53	84.85	87.98	86.41	85.33

Table 6. Performance after removing different deep learning components of our architecture for multi-modal model. e presents excluding the respective component of our architecture. Bold colored row presents the whole architecture’s performance.

7 Opportunities and Future Work

Accurate recognition of social interactions in naturalistic settings enables applications across mental health, physical health and wellness, and human-centered computing. By demonstrating that interactions can be detected using lightweight, on-device sensing without storing raw audio, this work lowers barriers to deploying interaction-aware systems in real-world settings where privacy, battery life, and user burden are critical constraints.

Clinical Applications in Mental Health. Our system provides a scalable tool for researchers studying social interaction patterns and their associations with mental and physical health outcomes (e.g., [35, 53, 54]). With a balanced accuracy of 90.36%, the system captures the majority of users’ interactions, enabling longitudinal measurement at a temporal resolution that is difficult to achieve using retrospective self-report alone. This capability supports applications such as monitoring social engagement and providing feedback to facilitate reflection or behavior change [61].

The system’s duty-cycled design further enables timely, context-aware interventions. Interaction-aware triggers could be used to prompt skill use or deliver support during or immediately following social interactions. By

incorporating multimodal cues beyond foreground speech and not requiring speech in every sensing window, the system may be particularly well suited for populations, such as individuals with social anxiety, for whom interactions may involve limited speech or extended silence, especially during early stages of exposure-based interventions [11, 28, 41].

User Experience Applications. Beyond clinical and research use, our findings have implications for smartwatch user experience design. Lightweight, on-device interaction detection enables notification and survey scheduling that respects social context without continuous sensing. For example, systems can defer interruptions until an interaction has concluded, reducing disruption and improving long-term usability and engagement.

Future Directions. Future work includes incorporating adaptive, user-specific thresholds; exploring richer yet privacy-preserving representations of social context; and validating the system across more diverse populations and environments. Integrating interaction detection with complementary self-report or contextual signals may further enable assessment not only of when interactions occur, but also how they are experienced.

8 Limitations

This work has several limitations that reflect deliberate design tradeoffs, as well as opportunities for future research. To prioritize privacy and participant comfort, our system does not store or transmit raw audio. All processing is performed on-device, and only derived features (e.g., log-mel spectrograms, foreground speech estimates, and interaction cues) are retained. While this design substantially reduces privacy risk, it limits the range of social interactions and analyses that can be supported. In particular, the system is designed to detect interactions that are at least partially audio-based and does not capture text-based social interactions (e.g., texting or messaging on social media) or non-audio communication modalities (e.g., sign language). Similarly, applications requiring access to semantic content, prosody, sentiment, or fine-grained conversational dynamics are not feasible with the current system.

The system also relies on duty-cycled rather than continuous audio sensing. Although the 1.5-minute duty cycle balances privacy, battery consumption, and detection performance, it may miss brief interactions or interactions occurring entirely between probe windows. While our evaluation demonstrates high recall for interactions of typical duration in naturalistic settings, applications requiring exhaustive capture may benefit from adaptive or continuous sensing strategies. Additionally, the current system could benefit from personalized adaptations to individual differences in speaking style, interaction patterns, or device placement in future work.

Finally, the evaluation was conducted primarily with participants from a single large public university. Although the sample included variation in age, roles, and daily routines, social interaction patterns and smartwatch usage may differ in other demographic, occupational, or cultural contexts. Further studies are needed to assess generalizability across more diverse populations and settings.

9 Conclusion

We presented the first privacy-preserving, multimodal framework for detecting social interactions using off-the-shelf smartwatches. The system combines duty-cycled acoustic sensing with inertial and physiological signals, along with lightweight on-device modeling to accurately identify interactions without storing or transmitting raw audio. To validate this approach, we conducted a real-world deployment with 38 participants wearing the smartwatch during their daily activities, yielding over 900 hours of data and thousands of annotated interaction events. Through extensive evaluation, we demonstrated that multimodal sensing substantially improves interaction detection performance, achieving balanced accuracy exceeding 90% while remaining computationally efficient and suitable for on-watch inference. By showing that reliable social interaction detection is possible under strict privacy, resource, and user-burden constraints, this work advances the design of scalable, social interaction-aware systems and opens new opportunities for applications in mental health, human-centered computing, and beyond.

References

- [1] Md Sabbir Ahmed, Noah French, Mark Rucker, Zhiyuan Wang, Taylor Myers-Brower, Kaitlyn Petz, Mehdi Boukhechba, Bethany A. Teachman, and Laura E. Barnes. 2025. WatchAnxiety: A Transfer Learning Approach for State Anxiety Prediction from Smartwatch Data. *2025 IEEE 21st International Conference on Body Sensor Networks (BSN)* (Nov. 2025), 1–4. <https://doi.org/10.1109/bsn66969.2025.11337873>
- [2] Md Sabbir Ahmed, Arafat Rahman, Zhiyuan Wang, Mark Rucker, and Laura E. Barnes. 2024. A Resource Efficient System for On-Smartwatch Audio Processing. *Proceedings of the 30th Annual International Conference on Mobile Computing and Networking* (Dec. 2024), 1805–1807. <https://doi.org/10.1145/3636534.3698866>
- [3] Mohsin Y Ahmed, Sean Kenkeremath, and John Stankovic. 2015. SocialSense: A collaborative mobile platform for speaker and mood identification. In *Lecture Notes in Computer Science*. Springer International Publishing, Cham, 68–83.
- [4] Tuka AlHanai and Mohammad Ghassemi. 2017. Predicting Latent Narrative Mood Using Audio and Physiologic Data. *Proceedings of the AAAI Conference on Artificial Intelligence* 31, 1 (Feb. 2017). <https://doi.org/10.1609/aaai.v31i1.10625>
- [5] Apple Inc. n.d.. Track your sleep with Apple Watch. Apple Support. <https://support.apple.com/en-gb/guide/watch/apd830528336/watchos>.
- [6] Rummana Bari, Roy J Adams, Md Mahbubur Rahman, Megan Battles Parsons, Eugene H Buder, and Santosh Kumar. 2018. rConverse: Moment by moment conversation detection using a mobile respiration sensor. *Proc. ACM Interact. Mob. Wearable Ubiquitous Technol.* (2018).
- [7] Rummana Bari, Md Mahbubur Rahman, Nazir Saleheen, Megan Battles Parsons, Eugene H Buder, and Santosh Kumar. 2020. Automated detection of stressful conversations using wearable physiological and inertial sensors. *Proc. ACM Interact. Mob. Wearable Ubiquitous Technol.* 4, 4 (2020), 1–23.
- [8] George Boateng, Prabhakaran Santhanam, Janina Lüscher, Urte Scholz, and Tobias Kowatsch. 2019. VADLite: An open-source lightweight system for real-time voice activity detection on smartwatches. In *Adjunct Proc. of 2019 ACM UbiComp-ISWC*.
- [9] Tanzeem Choudhury and Alex Pentland. 2004. Characterizing social interactions using the sociometer. In *Proceedings of NAACOS*. 1–4.
- [10] Gus Cooney, Adam M Mastroianni, Nicole Abi-Esber, and Alison Wood Brooks. 2020. The many minds problem: disclosure in dyadic versus group conversation. *Current Opinion in Psychology* 31 (Feb. 2020), 22–27. <https://doi.org/10.1016/j.copsyc.2019.06.032>
- [11] Brechtje de Mooij, Minne Fekkes, Anne C. Miers, Alithe L. van den Akker, Ron H. J. Scholte, and Geertjan Overbeek. 2023. What Works in Preventing Emerging Social Anxiety: Exposure, Cognitive Restructuring, or a Combination? *Journal of Child and Family Studies* 32, 2 (Jan. 2023), 498–515. <https://doi.org/10.1007/s10826-023-02536-w>
- [12] Android Developers. 2024. Batching. (2024). <https://source.android.com/docs/core/interaction/sensors/batching> Accessed: 2026-01-17.
- [13] Android Developers. 2025. AlarmManager. (2025). <https://developer.android.com/reference/android/app/AlarmManager> Accessed: 2026-01-18.
- [14] Android Developers. 2025. Monitoring Sensor Events. https://developer.android.com/develop/sensors-and-location/sensors/sensors_overview#sensors-monitor
- [15] Android Developers. 2025. Sensor stack. <https://source.android.com/docs/core/interaction/sensors/sensor-stack>
- [16] Google Developers. 2025. Audio classification guide. https://ai.google.dev/edge/mediapipe/solutions/audio/audio_classifier Accessed: 2026-01-16.
- [17] Andreas Ebbelohj, Mette Østergaard Thunbo, Ole Emil Andersen, Michala Vilstrup Glindtvaad, and Adam Hulman. 2022. Transfer learning for non-image data in clinical research: A scoping review. *PLOS Digital Health* 1, 2 (Feb. 2022), e0000014. <https://doi.org/10.1371/journal.pdig.0000014>
- [18] Denzil Ferreira and Raghu Mulukutla. 2020. AWARE Plugin: Conversations. https://github.com/denzilferreira/com.aware.plugin.studentlife.audio_final. (2020). Accessed: 2025-05-30.
- [19] Fitbit. n.d.. Breathing rate. Fitbit.com. <https://dev.fitbit.com/build/reference/web-api/breathing-rate/>.
- [20] Jort F. Gemmeke, Daniel P. W. Ellis, Dylan Freedman, Aren Jansen, Wade Lawrence, R. Channing Moore, Manoj Plakal, and Marvin Ritter. 2017. Audio Set: An ontology and human-labeled dataset for audio events. *2017 IEEE International Conference on Acoustics, Speech and Signal Processing (ICASSP)* (March 2017). <https://doi.org/10.1109/icassp.2017.7952261>
- [21] Diane Carol Gooding and Madeline Pflum. 2022. The Transdiagnostic Nature of Social Anhedonia: Historical and Current Perspectives. *Anhedonia: Preclinical, Translational, and Clinical Integration* (2022), 381–395. https://doi.org/10.1007/7854_2021_301
- [22] Google. 2017. AudioSet. <https://research.google.com/audioset/>
- [23] Aurélien Géron. 2019. *Hands-on machine learning with Scikit-Learn and TensorFlow concepts, tools, and techniques to build intelligent systems* (2 ed.). O'Reilly Media, Inc.
- [24] Kaiming He, Xiangyu Zhang, Shaoqing Ren, and Jian Sun. 2016. Deep Residual Learning for Image Recognition. In *Proceedings of the IEEE Conference on Computer Vision and Pattern Recognition (CVPR)*.
- [25] Andrew G. Howard, Menglong Zhu, Bo Chen, Dmitry Kalenichenko, Weijun Wang, Tobias Weyand, Marco Andreetto, and Hartwig Adam. 2017. MobileNets: Efficient Convolutional Neural Networks for Mobile Vision Applications. (2017). arXiv:1704.04861 [cs.CV] <https://arxiv.org/abs/1704.04861>

- [26] Nicholas Hutchins, Andrew Allen, Michelle Curran, and Lee Kannis-Dymand. 2021. Social anxiety and online social interaction. *Australian Psychologist* 56, 2 (March 2021), 142–153. <https://doi.org/10.1080/00050067.2021.1890977>
- [27] Katrin Hänsel, Kleomenis Katevas, Guido Orgs, Daniel C. Richardson, Akram Alomainy, and Hamed Haddadi. 2018. The potential of wearable technology for monitoring social interactions based on interpersonal synchrony. *Proceedings of the 4th ACM Workshop on Wearable Systems and Applications* (2018), 45–47. <https://doi.org/10.1145/3211960.3211979>
- [28] Isabel L. Kampmann, Paul M.G. Emmelkamp, Dwi Hartanto, Willem-Paul Brinkman, Bonne J.H. Zijlstra, and Nexhmedin Morina. 2016. Exposure to virtual social interactions in the treatment of social anxiety disorder: A randomized controlled trial. *Behaviour Research and Therapy* 77 (Feb. 2016), 147–156. <https://doi.org/10.1016/j.brat.2015.12.016>
- [29] Kleomenis Katevas, Katrin Hänsel, Richard Clegg, Ilias Leontiadis, Hamed Haddadi, and Laurissa Tokarchuk. 2019. Finding Dory in the Crowd: Detecting Social Interactions using Multi-Modal Mobile Sensing. *Proceedings of the 1st Workshop on Machine Learning on Edge in Sensor Systems* (Nov. 2019), 37–42. <https://doi.org/10.1145/3362743.3362959>
- [30] Christine E. King and Majid Sarrafzadeh. 2017. A Survey of Smartwatches in Remote Health Monitoring. *Journal of Healthcare Informatics Research* 2, 1–2 (Dec. 2017), 1–24. <https://doi.org/10.1007/s41666-017-0012-7>
- [31] Hyeokhyen Kwon, Catherine Tong, Harish Haresamudram, Yan Gao, Gregory D. Abowd, Nicholas D. Lane, and Thomas Plötz. 2020. IMUTube. *Proceedings of the ACM on Interactive, Mobile, Wearable and Ubiquitous Technologies* 4, 3 (2020), 1–29. <https://doi.org/10.1145/3411841>
- [32] Nicholas Lane, Mashfiqui Mohammad, Mu Lin, Xiaochao Yang, Hong Lu, Shahid Ali, Afsaneh Doryab, Ethan Berke, Tanzeem Choudhury, and Andrew Campbell. 2011. BeWell: A Smartphone Application to Monitor, Model and Promote Wellbeing. *Proceedings of the 5th International ICST Conference on Pervasive Computing Technologies for Healthcare* (2011). <https://doi.org/10.4108/icst.pervasivehealth.2011.246161>
- [33] Scikit learn developers. [n. d.]. NearestCentroid. <https://scikit-learn.org/stable/modules/generated/sklearn.neighbors.NearestCentroid.html> Accessed: 2026-01-20.
- [34] Matthew Lehet, Meisam K. Arjmandi, Derek Houston, and Laura Dilley. 2020. Circumspection in using automated measures: Talker gender and addressee affect error rates for adult speech detection in the Language ENvironment Analysis (LENA) system. *Behavior Research Methods* 53, 1 (2020), 113–138. <https://doi.org/10.3758/s13428-020-01419-y>
- [35] N. Leigh-Hunt, D. Bagguley, K. Bash, V. Turner, S. Turnbull, N. Valtorta, and W. Caan. 2017. An overview of systematic reviews on the public health consequences of social isolation and loneliness. *Public Health* 152 (Nov. 2017), 157–171. <https://doi.org/10.1016/j.puhe.2017.07.035>
- [36] Stephen C. Levinson. 2016. Turn-taking in Human Communication – Origins and Implications for Language Processing. *Trends in Cognitive Sciences* 20, 1 (Jan. 2016), 6–14. <https://doi.org/10.1016/j.tics.2015.10.010>
- [37] Stephen C. Levinson. 2025. The Interaction Engine. (May 2025). <https://doi.org/10.1017/9781009570343>
- [38] Dawei Liang, Zifan Xu, Yinuo Chen, Rebecca Adaimi, David Harwath, and Edison Thomaz. 2023. A Dataset for Foreground Speech Analysis With Smartwatches In Everyday Home Environments. *2023 IEEE International Conference on Acoustics, Speech, and Signal Processing Workshops (ICASSPW)* (2023), 1–5. <https://doi.org/10.1109/icasspw59220.2023.10192949>
- [39] Dawei Liang, Alice Zhang, and Edison Thomaz. 2023. Automated face-to-face conversation detection on a commodity smartwatch with acoustic sensing. *Proc. ACM Interact. Mob. Wearable Ubiquitous Technol.* 7, 3 (2023), 1–29.
- [40] Nathan Liang, Samantha J Grayson, Mia A Kussman, Judith N Mildner, and Diana I Tamir. 2024. In-person and virtual social interactions improve well-being during the COVID-19 pandemic. *Comput. Hum. Behav. Rep.* 15, 100455 (2024), 100455.
- [41] Xiangting Bernice Lin, Tih-Shih Lee, Yin Bun Cheung, Joanna Ling, Shi Hui Poon, Leslie Lim, Hai Hong Zhang, Zheng Yang Chin, Chuan Chu Wang, Ranga Krishnan, and Cuntai Guan. 2019. Exposure Therapy With Personalized Real-Time Arousal Detection and Feedback to Alleviate Social Anxiety Symptoms in an Analogue Adult Sample: Pilot Proof-of-Concept Randomized Controlled Trial. *JMIR Ment Health* 6, 6 (14 Jun 2019), e13869. <https://doi.org/10.2196/13869>
- [42] Paulo N Lopes, Marc A Brackett, John B Nezlek, Astrid Schütz, Ina Sellin, and Peter Salovey. 2004. Emotional intelligence and social interaction. *Personality and social psychology bulletin* 30, 8 (2004), 1018–1034.
- [43] Hong Lu, A J Bernheim Brush, Bodhi Priyantha, Amy K Karlson, and Jie Liu. 2011. SpeakerSense: Energy Efficient Unobtrusive Speaker Identification on Mobile Phones. In *Lecture Notes in Computer Science*.
- [44] Richard E Lucas, Carol Wallsworth, Ivana Anusic, and M Brent Donnellan. 2021. A direct comparison of the day reconstruction method (DRM) and the experience sampling method (ESM). *J. Pers. Soc. Psychol.* 120, 3 (2021), 816–835.
- [45] Chengwen Luo and Mun Choon Chan. 2013. SocialWeaver: Collaborative Inference of Human Conversation Networks Using Smartphones. *Proceedings of the 11th ACM Conference on Embedded Networked Sensor Systems* (Nov. 2013), 1–14. <https://doi.org/10.1145/2517351.2517353>
- [46] Alessandra Mabeth, Michelle R. Bruni, Brittanny De La Cruz, Jacqueline A. Erens, Natsuki Atagi, Megan L. Robbins, Christine Chiarello, and Jessica L. Montag. 2022. Using the Electronically Activated Recorder (EAR) to Capture the Day-to-Day Linguistic Experiences of Young Adults. *Collabra: Psychology* 8, 1 (2022). <https://doi.org/10.1525/collabra.36310>
- [47] Dominique Makowski, Tam Pham, Zen J. Lau, Jan C. Brammer, François Lespinasse, Hung Pham, Christopher Schölzel, and S. H. Annabel Chen. 2021. NeuroKit2: A Python toolbox for neurophysiological signal processing. *Behavior Research Methods* 53, 4 (feb 2021), 1689–1696.

- <https://doi.org/10.3758/s13428-020-01516-y>
- [48] Adam M. Mastroianni, Daniel T. Gilbert, Gus Cooney, and Timothy D. Wilson. 2021. Do conversations end when people want them to? *Proceedings of the National Academy of Sciences* 118, 10 (March 2021). <https://doi.org/10.1073/pnas.2011809118>
- [49] Shoba S. Meera, Divya Swaminathan, Sri Ranjani Venkata Murali, Reny Raju, Malavi Srikar, Sahana Shyam Sundar, Senthil Amudhan, Alejandrina Cristia, Rahul Pawar, Achuth Rao, Prathyusha P. Vasuki, Shree Volme, and Ashok Mysore. 2025. Validation of the Language ENvironment Analysis (LENA) Automated Speech Processing Algorithm Labels for Adult and Child Segments in a Sample of Families From India. *Journal of Speech, Language, and Hearing Research* 68, 1 (Jan. 2025), 40–53.
- [50] Matthias R. Mehl. 2017. The Electronically Activated Recorder (EAR). *Current Directions in Psychological Science* 26, 2 (April 2017), 184–190. <https://doi.org/10.1177/0963721416680611>
- [51] Marije Michel and Marco Cappellini. 2019. Alignment During Synchronous Video Versus Written Chat L2 Interactions: A Methodological Exploration. *Annual Review of Applied Linguistics* 39 (March 2019), 189–216. <https://doi.org/10.1017/s0267190519000072>
- [52] Amrutha Nadarajan, Krishna Somandepalli, and Shrikanth S. Narayanan. 2019. Speaker Agnostic Foreground Speech Detection from Audio Recordings in Workplace Settings from Wearable Recorders. *ICASSP 2019 - 2019 IEEE International Conference on Acoustics, Speech and Signal Processing (ICASSP)* (May 2019), 6765–6769. <https://doi.org/10.1109/icassp.2019.8683244>
- [53] Eisuke Ono, Takayuki Nozawa, Taiki Ogata, Masanari Motohashi, Naoki Higo, Tetsuro Kobayashi, Kunihiro Ishikawa, Koji Ara, Kazuo Yano, and Yoshihiro Miyake. 2011. Relationship between social interaction and mental health. In *2011 IEEE/SICE International Symposium on System Integration (SII)*. IEEE, 246–249.
- [54] Mark C Pachucki, Emily J Ozer, Alain Barrat, and Ciro Cattuto. 2015. Mental health and social networks in early adolescence: A dynamic study of objectively-measured social interaction behaviors. *Social science & medicine* 125 (2015), 40–50.
- [55] Ernest S Park and Verlin B Hinsz. 2015. Group interaction sustains positive moods and diminishes negative moods. *Group dynamics: Theory, research, and practice* 19, 4 (2015), 290.
- [56] Ji Soo Park, Sa-Yoon Park, Jae Won Moon, Kwangsoo Kim, and Dong In Suh. 2025. Artificial Intelligence Models for Pediatric Lung Sound Analysis: Systematic Review and Meta-Analysis. *J Med Internet Res* 27 (18 Apr 2025), e66491. <https://doi.org/10.2196/66491>
- [57] Leonard S. Peperkoorn, D. Vaughn Becker, Daniel Balliet, Simon Columbus, Catherine Molho, and Paul A. M. Van Lange. 2020. The prevalence of dyads in social life. *PLOS ONE* 15, 12 (Dec. 2020), e0244188. <https://doi.org/10.1371/journal.pone.0244188>
- [58] Manoj Plakal and Dan Ellis. 2019. YAMNet. <https://github.com/tensorflow/models/tree/master/research/audioset/yamnet>
- [59] Aditya Ponnada, Caitlin Haynes, Dharam Maniar, Justin Manjourides, and Stephen Intille. 2017. Microinteraction Ecological Momentary Assessment Response Rates. *Proceedings of the ACM on Interactive, Mobile, Wearable and Ubiquitous Technologies* 1, 3 (2017), 1–16. <https://doi.org/10.1145/3130957>
- [60] Mashfiqui Rabbi, Shahid Ali, Tanzeem Choudhury, and Ethan Berke. 2011. Passive and In-Situ assessment of mental and physical well-being using mobile sensors. *Proceedings of the 13th international conference on Ubiquitous computing* (2011), 385–394. <https://doi.org/10.1145/2030112.2030164>
- [61] Mashfiqui Rabbi, Min Hane Aung, Mi Zhang, and Tanzeem Choudhury. 2015. MyBehavior: automatic personalized health feedback from user behaviors and preferences using smartphones. In *Proceedings of the 2015 ACM international joint conference on pervasive and ubiquitous computing*. 707–718.
- [62] Md Mahbubur Rahman, Amin Ahsan Ali, Kurt Plarre, Mustafa al’Absi, Emre Ertin, and Santosh Kumar. 2011. mConverse: Inferring conversation episodes from respiratory measurements collected in the field. In *Proceedings of the 2nd Conference on Wireless Health*. 1–10.
- [63] Madeleine Rassaby, Isabella G. Spaulding, and Charles T. Taylor. 2024. Fear of positive evaluation and social affiliation in social anxiety disorder and major depression. *Journal of Anxiety Disorders* 107 (2024), 102931. <https://doi.org/10.1016/j.janxdis.2024.102931>
- [64] Jeffrey A. Richards, Dongxin Xu, and Jill Gilkerson. 2010. *Development and Performance of the LENA Automatic Autism Screen*. Technical Report. LENA Foundation.
- [65] Yannick Roos, Michael D Krämer, David Richter, Ramona Schoedel, and Cornelia Wrzus. 2023. Does your smartphone “know” your social life? A methodological comparison of day reconstruction, experience sampling, and mobile sensing. *Adv. Methods Pract. Psychol. Sci.* 6, 3 (2023).
- [66] Hope Schroeder, Deb Roy, and Jad Kabbara. 2024. Fora: A corpus and framework for the study of facilitated dialogue. In *Proceedings of the 62nd Annual Meeting of the Association for Computational Linguistics (Volume 1: Long Papers)*, Lun-Wei Ku, Andre Martins, and Vivek Srikumar (Eds.). Association for Computational Linguistics, Bangkok, Thailand, 13985–14001. <https://doi.org/10.18653/v1/2024.acl-long.754>
- [67] Andreas Schwerdtfeger and Peter Friedrich-Mai. 2009. Social interaction moderates the relationship between depressive mood and heart rate variability: evidence from an ambulatory monitoring study. *Health Psychol.* (2009).
- [68] Farhad Shahmohammadi, Anahita Hosseini, Christine E King, and Majid Sarrafzadeh. 2017. Smartwatch based activity recognition using active learning. In *2017 IEEE/ACM CHASE*. IEEE, 321–329.
- [69] Sara Shahrestani, Elizabeth M Stewart, Daniel S Quintana, Ian B Hickie, and Adam J Guastella. 2015. Heart rate variability during adolescent and adult social interactions: A meta-analysis. *Biol. Psychol.* 105 (2015), 43–50.

- [70] Jessie Sun, Kelci Harris, and Simine Vazire. 2020. Is well-being associated with the quantity and quality of social interactions? *Journal of personality and social psychology* 119, 6 (2020), 1478.
- [71] Rui Wang, Fanglin Chen, Zhenyu Chen, Tianxing Li, Gabriella Harari, Stefanie Tignor, Xia Zhou, Dror Ben-Zeev, and Andrew T. Campbell. 2014. StudentLife: assessing mental health, academic performance and behavioral trends of college students using smartphones. *Proceedings of the 2014 ACM International Joint Conference on Pervasive and Ubiquitous Computing* (2014), 3–14. <https://doi.org/10.1145/2632048.2632054>
- [72] Wikipedia contributors. 2025. Samsung Galaxy Watch 5. https://en.wikipedia.org/wiki/Samsung_Galaxy_Watch_5. Accessed: 2026-01-21.
- [73] Dongxin Xu, Umit Yapanel, Sharmistha Gray, Jill Gilkerson, Jeffrey Richards, and John Hansen. 2008. Signal processing for young child speech language development. In *The 1st Workshop on Child, Computer, and Interaction*. <https://api.semanticscholar.org/CorpusID:21425835>
- [74] Michael Yeomans, F. Katelynn Boland, Hanne K. Collins, Nicole Abi-Esber, and Alison Wood Brooks. 2023. A Practical Guide to Conversation Research: How to Study What People Say to Each Other. *Advances in Methods and Practices in Psychological Science* 6, 4 (Oct. 2023). <https://doi.org/10.1177/25152459231183919>
- [75] Alice Zhang, Callihan Bertley, Dawei Liang, and Edison Thomaz. 2025. Detecting In-Person Conversations in Noisy Real-World Environments with Smartwatch Audio and Motion Sensing. (2025). <https://doi.org/10.48550/ARXIV.2507.12002>
- [76] Ruixue Zhaoyang, Martin J. Sliwinski, Lynn M. Martire, and Joshua M. Smyth. 2018. Age differences in adults' daily social interactions: An ecological momentary assessment study. *Psychology and Aging* 33, 4 (2018), 607–618. <https://doi.org/10.1037/pag0000242>